

See discussions, stats, and author profiles for this publication at: <https://www.researchgate.net/publication/236082381>

Fragment-Based Drug Discovery of 2-Thiazolidinones as Inhibitors of the Histone Reader BRD4 Bromodomain

ARTICLE in JOURNAL OF MEDICINAL CHEMISTRY · MARCH 2013

Impact Factor: 5.45 · DOI: 10.1021/jm301793a · Source: PubMed

CITATIONS

38

READS

73

16 AUTHORS, INCLUDING:



Yechun Xu

Shanghai Institute of Materia Medica

73 PUBLICATIONS 1,270 CITATIONS

SEE PROFILE



Xin Wang

Nanjing University of Science and Technology

951 PUBLICATIONS 11,542 CITATIONS

SEE PROFILE



Bing Xiong

Shanghai Institute of Materia Medica

67 PUBLICATIONS 825 CITATIONS

SEE PROFILE



Naixia Zhang

University of Minnesota Twin Cities

38 PUBLICATIONS 865 CITATIONS

SEE PROFILE

Fragment-Based Drug Discovery of 2-Thiazolidinones as Inhibitors of the Histone Reader BRD4 Bromodomain

Lele Zhao,^{†,||} Danyan Cao,^{†,||} Tiantian Chen,^{†,||} Yingqing Wang,^{‡,||} Zehong Miao,[‡] Yechun Xu,[†] Wuyan Chen,[†] Xin Wang,[†] Yanlian Li,[†] Zhiyan Du,[†] Bing Xiong,^{*,†} Jian Li,[§] Chunyan Xu,[§] Naixia Zhang,[†] Jianhua He,^{*,§} and Jingkang Shen^{*,†}

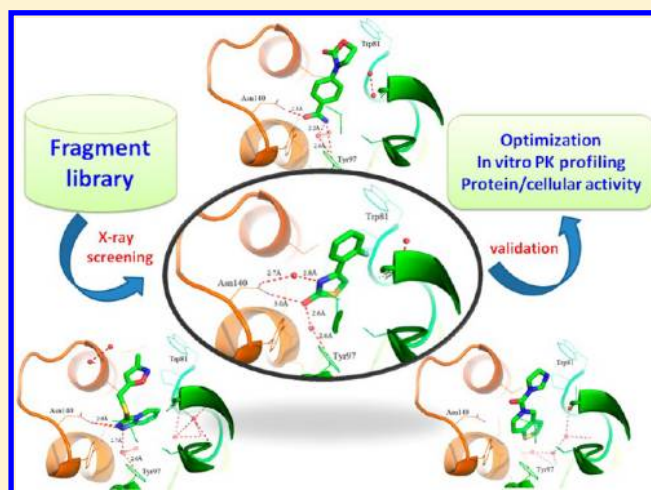
[†]Department of Medicinal Chemistry, State Key Laboratory of Drug Research, Shanghai Institute of Materia Medica, Chinese Academy of Sciences, 555 Zuchongzhi Road, Shanghai 201203, China

[‡]Division of Anti-Tumor Pharmacology, State Key Laboratory of Drug Research, Shanghai Institute of Materia Medica, Chinese Academy of Sciences, 555 Zuchongzhi Road, Shanghai 201203, China

[§]Shanghai Institute of Applied Physics, Chinese Academy of Sciences, 239 Zhangheng Road, Shanghai 201204, China

S Supporting Information

ABSTRACT: Recognizing acetyllysine of histone is a vital process of epigenetic regulation that is mediated by a protein module called bromodomain. To contribute novel scaffolds for developing into bromodomain inhibitors, we utilize a fragment-based drug discovery approach. By successively applying docking and X-ray crystallography, we were able to identify 9 fragment hits from diffracting more than 60 crystals. In the present work, we described four of them and carried out the integrated lead optimization for fragment 8, which bears a 2-thiazolidinone core. After several rounds of structure guided modifications, we assessed the druggability of 2-thiazolidinone by modulating in vitro pharmacokinetic studies and cellular activity assay. The results showed that two potent compounds of 2-thiazolidinones have good metabolic stability. Also, the cellular assay confirmed the activities of 2-thiazolidinones. Together, we hope the identified 2-thiazolidinone chemotype and other fragment hits described herein can stimulate researchers to develop more diversified bromodomain inhibitors.



■ INTRODUCTION

Epigenetic regulation of gene expression is currently the focus of intensive research in the postgenomic era. At the molecular level, epigenetic regulation involves dynamic and reversible modification of DNA and the proteins that package DNA.¹ Histones, the core proteins within chromatin structure, are subjected to a range of post-translational modifications (PTMs), mainly including acetylation, methylation, phosphorylation, and ubiquitination.² The combinatorial characterized covalent modification on the histone tails is coined "histone code",³ which is believed to be key to understanding the gene expression pattern and many heritable changes in phenotype that are not encoded in the underlying DNA sequences. This histone code hypothesis has led to the presumption that there must be protein families for specifically adding, removing, and recognizing the PTM marks. In recent years, all three types of proteins have been identified for lysine acetylation. For example, histone acetyltransferases (HATs) act as a writer to transfer the acetyl group from acetyl CoA to form an ϵ -N-acetyllysine, whereas histone deacetylases (HDACs) work as an eraser to remove the acetyl group from the

histone tail. The proteins containing bromodomains could bind to the acetylated lysine (KAc) and are playing just as readers for signaling transduction of the lysine acetylation states of histone. The aberrant events involved in writer–reader–eraser processes have been associated with many human diseases, especially certain cancers.⁴

Bromodomain, a protein module containing approximately 110 amino acids, has been observed as part of numerous, large protein architectures, many of which are regulators of gene transcription such as HATs, components of chromatin-remodeling complexes, and methyltransferases.⁵ It has been recently established that BRD4, a member of bromodomain and extra-terminal (BET) family, is a critical mediator of transcriptional elongation by recruiting the positive transcription elongation factor complex (P-TEFb).⁶ Since cyclin-dependent kinase 9, the core component of P-TEFb, is a validated target for chronic lymphocytic leukemia, it was proposed that BRD4 is a

Received: December 5, 2012

Published: March 26, 2013

compelling target for cancer.⁷ Importantly, BRD4 has been identified as a component of recurrent chromosomal translocation in an aggressive form of human squamous carcinoma by expressing the tandem N-terminal bromodomains of BRD4 as an in-frame chimera with the NUT (nuclear protein in testis).⁸ RNAi silencing of BRD4-NUT arrests proliferation and prompts terminal squamous differentiation. These observations underscore the potential therapeutic role of inhibitors for the proteins containing BRDs such as BRD4.⁹

The majority of efforts on developing small molecules as BRD inhibitors have been focused on the BET family.¹⁰ Currently, only limited chemotypes have been reported to block the signaling transduction of bromodomains of BET members that interact with the acetylated histone. The first potent BRD inhibitors **1** and **2** were discovered independently by two groups,^{7,11} and both compounds contain the diazepine core that is commonly found in CNS drugs such as alprazolam and triazolam. (+)-JQ1, identified by Bradner's group guided by a docking study on the compounds disclosed in a patent filed by Mitsubishi Pharmaceuticals, is a potent and selective BET family inhibitor with a K_d of ~ 50 nM to the first bromodomain of BRD4 (BRD4(I)). Further studies showed that the competitive binding of JQ1 to the bromodomain displaces the BRD4 fusion oncoprotein from chromatin, prompting squamous differentiation and specific antiproliferative effects in BRD4-dependent cell lines and patient-derived xenograft models. Later, they discovered a new application of JQ1 in a putative male contraception by affecting another BET family member BRDT.¹² Compound **2** (I-BET762), discovered by Nicodeme et al.^{11b} from GlaxoSmithKline (GSK), contains a very similar scaffold to JQ1. I-BET762 was initially developed as a new generation of immunomodulatory drugs and is now entering phase I clinical trials for the potential treatment of testis (NUT) midline carcinoma (NMC).¹³ In 2011, researchers at the University of Oxford and GSK simultaneously disclosed a new chemotype, 3,5-dimethylisoxazole such as IBET151 (**3**, shown in Figure 1), acting as a KAc mimic to inhibit bromodomains.¹⁴ By utilizing the effective fragment-based drug discovery (FBDD)

approach, Chung et al. were the first to identify the small weakly acting fragment and finally obtained a potent and selective inhibitor (compound **4**) of BRD2 bromodomain I ($K_d \approx 500$ nM) through extensive medicinal chemistry optimization.¹⁵

In the present work, we initialized an FBDD project with the aim to discover novel BRD4 inhibitors. On the basis of a computational docking study employing our own fragment library, we selected 41 fragments and utilized an X-ray crystallography approach to screen the fragments while simultaneously obtaining the binding conformation of the fragments to BRD4. Several hit fragments were identified after the structures of the complexes were solved. One of the fragments with a 2-thiazolidinone core was further optimized, based on the interaction information revealed by the crystal structures. Exploring the structure–activity relationship of 2-thiazolidinones resulted in a novel and potent BRD4 inhibitor with $IC_{50} \approx 0.3 \mu M$, equipotent to compound **4**. The in vitro pharmacokinetic study showed that this series has good potential for further drug development. Also, the cellular assays demonstrated that 2-thiazolidinones of BRD4 inhibitors have apparent proliferation inhibition in HT-29 cells and can reduce the expression of *c-myc* mRNA. Overall, we anticipate that the identified 2-thiazolidinone scaffold, together with other disclosed fragments, may aid in the design of new putative prototypes and stimulate other researchers to develop their own bromodomain inhibitors.

RESULTS AND DISCUSSION

Fragment Library. The fragment-based drug discovery involves the development of potent small-molecule ligands from low molecular weight fragment molecules.¹⁶ Therefore, the fragment library is the essential component of FBDD. Over the past decade, several approaches to construct the fragment library were proposed. The most familiar concept used in FBDD is the “rule of three”,¹⁷ which imitates the “rule of five” raised by Lipinski in 1997.¹⁸ Other approaches such as those of Chen and Hubbard at Vernalis¹⁹ and of Nunez et al.²⁰ were also described to build their fragment libraries. To build our own fragment library, initially all fragment compounds in ZINC database were downloaded from their Web site (<http://zinc.docking.org>) and filtered by the following rules:

- (1) molecular weight, ≤ 250 Da;
- (2) rotatable bonds, ≤ 5 ;
- (3) $\log P \leq 3.5$;
- (4) $1 \leq$ smallest set of smallest ring ≤ 4 .

Then the resulting fragments were further clustered into groups with a Tanimoto similarity of 0.7 as the cutoff by using Pipeline Pilot software. Subsequently, the compounds labeled as cluster center were selected as representative of these clusters. Finally 500 compounds were cherry-picked by human expertise and sent to chemical vendors for a purchase inquiry. 487 fragments are found in stock and consequently purchased. Some physicochemical properties of our fragment library are shown in Figure 2.

Library construction is not a “one size fits all” process. At Vernalis, as described by Chen and Hubbard,^{19a} they have evolved their first generation of fragment library from Ver2004 to Ver2008 by gradual inclusion of template fragments found in other projects or by removing unstable and/or low-hit-rate fragments. In our current library design, we are aware of some fragments that may be out of the range of the so-called “rule of three”. The main reason to do so is to assess which physicochemical properties of fragments are important for the

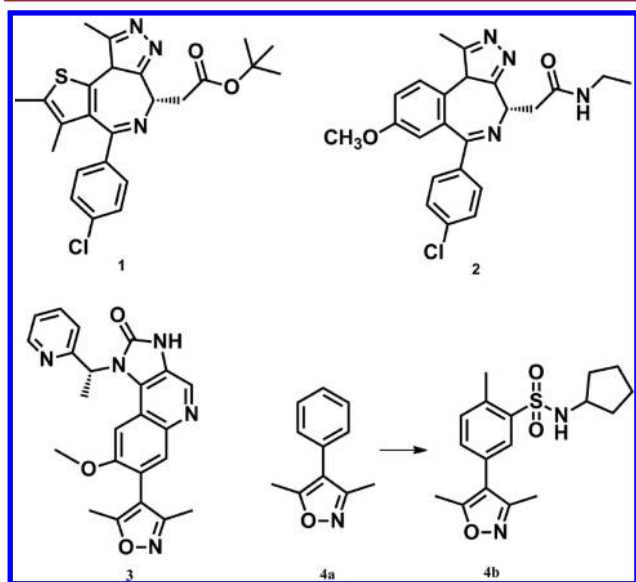


Figure 1. Representative inhibitors of bromodomains: **1**, (+)-JQ1; **2**, I-BET762; **3**, I-BET151; **4a**, 3,5-dimethyl-4-phenyloxazole; **4b**, N-cyclopentyl-3-(3,5-dimethylisoxazol-4-yl)benzenesulfonamide.

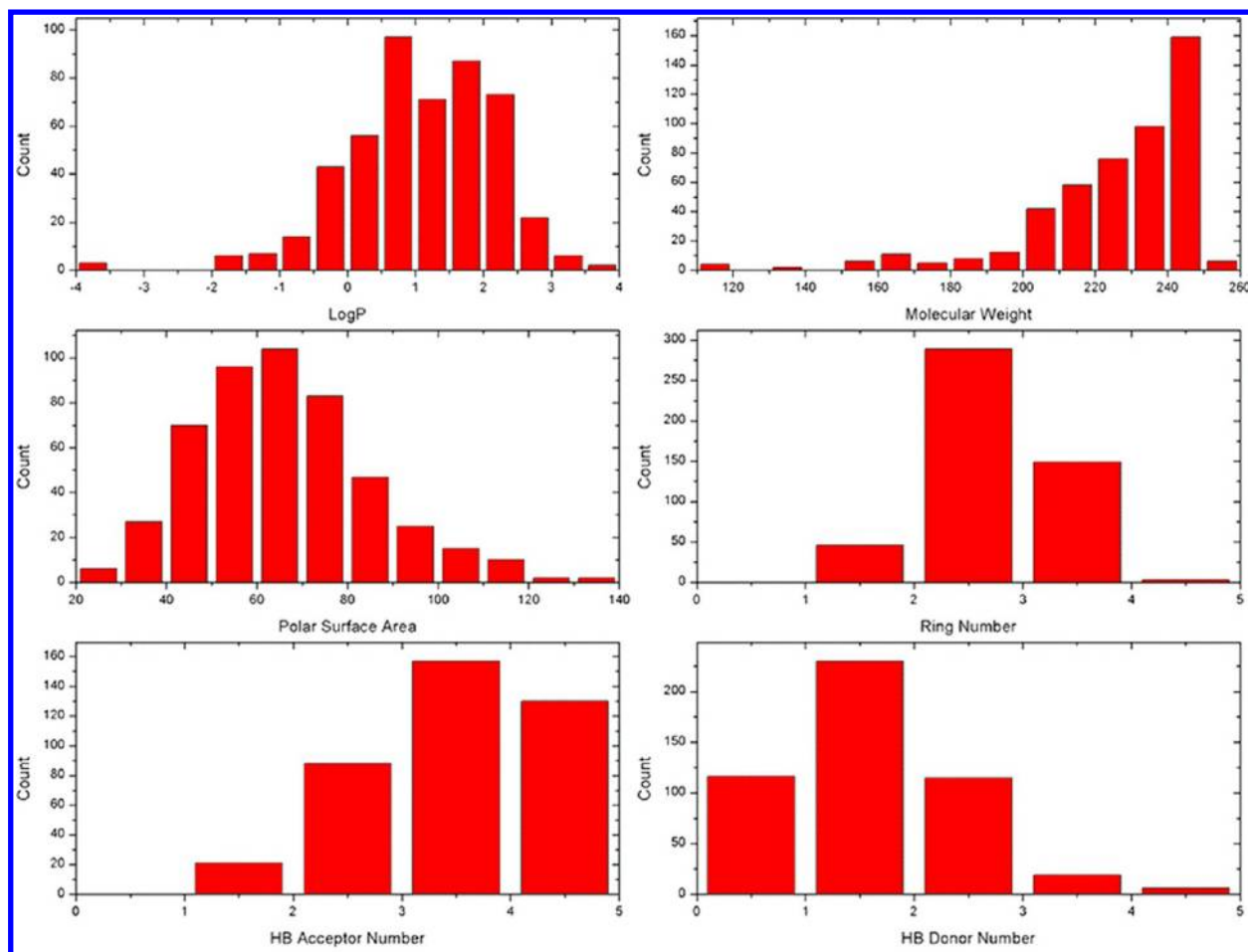


Figure 2. Physiochemical properties of our fragment library. The physiochemical properties including log *P*, molecular weight, polar surface area, ring number, hydrogen bond acceptor number, and donor number were calculated with ChemAxon software.²¹ The frequency of compounds within certain range of properties is depicted as histograms.

success of a fragment library. The information of which property is most relevant to the quality of the fragment library may be obtained after we screen our library within several projects. Such information may also prove to be beneficial for further extension of our library of compounds.

Hit Generation. Finding novel compounds as starting points for optimization is a major challenge in the drug discovery. Unlike high throughput screening, in FBDD the hits are low molecular weight fragments and the binding affinities of those fragments to the target are generally in the range 0.1–10 mM. Consequently, specialized biophysical tools for binding assay are needed to detect such weak binders,²² which consist of differential scanning fluorimetry (DSF),²³ ligand-detected NMR spectroscopy including the saturation transfer difference (STD) method,²⁴ water–ligand observed via gradient spectroscopy (WaterLOGSY)²⁵ and Carr–Purcell–Meiboom–Gill (CPMG) method,²⁶ surface plasmon resonance (SPR),²⁷ X-ray crystallography,²² molecular docking, and carefully designed biochemical screens.²⁸ It is more profitable to apply the fast and low-cost methods such as docking, DSF, ligand-based NMR methods, and the SPR method to enrich the promising hits. Then more accurate methods like protein-detected NMR and X-ray crystallography may be used to obtain detailed information of binding of fragment hits within the drug target. Although computer docking has limited ability of correctly scoring the molecules with weak interactions, it was utilized in the present

work to enrich the potential fragment hits to BRD4(I). There are several cocrystal structures of known bromodomain inhibitors with BRD4(I). We can thus grasp the essential clues about atomic interactions between BRD4(I) and its inhibitors. Such clues are helpful for hit ranking in docking studies and may overcome the limitation rooted in its inaccurate scoring function. The Glide program was utilized to dock molecules included in our fragment library to the BRD4(I) binding site based on the crystal structure of JQ1 in complex with BRD4(I). After the docking, all the binding conformations of fragments were checked for the interaction of the fragments with the conserved residue Asn140 in BRD4(I) binding site. Finally, 41 fragments were selected and processed for crystallization experiments. The direct X-ray crystallography screening has a unique advantage by providing validated, bona fide hits and simultaneously provides detailed atomic interaction information. To view the unambiguous recognition of the fragments in the binding site of BRD4(I), we used cocrystallization of the BRD4(I) protein with the fragments. More than 60 crystals grown from the cocrystallizations were diffracted, and data were collected at Shanghai Synchrotron Radiation Facility (SSRF). In the solved crystal structures, we were able to identify nine fragments in the binding site of BRD4(I) and four of them are illustrated in Figure 3. It thus demonstrated that the combination of computational molecular docking and directed X-ray crystallography is a promising screening method valuable to FBDD projects,

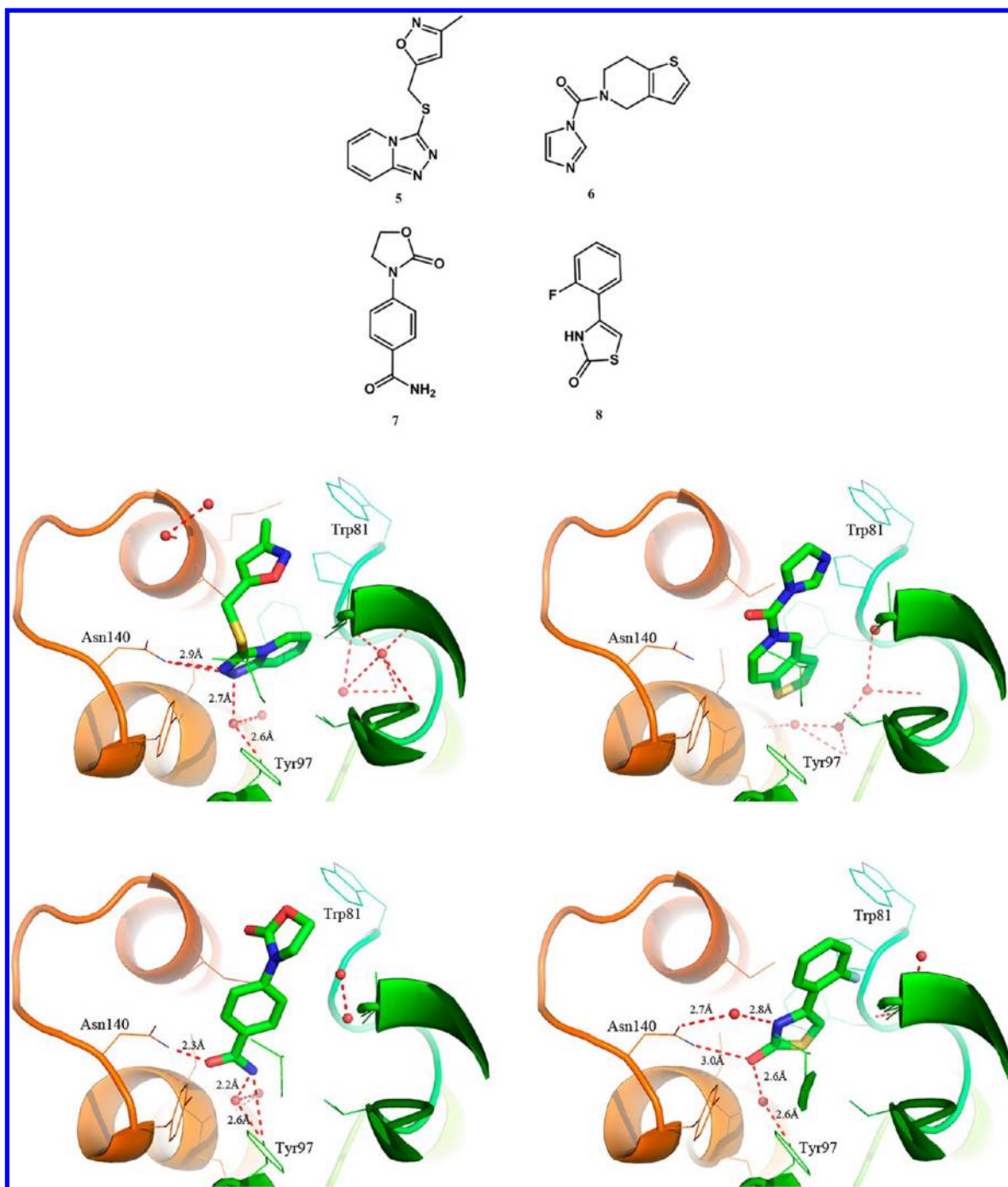


Figure 3. Cocystal structures of BRD4 bromodomain I and fragments 5–8. The fragments are shown in stick model, and BRD4(I) is shown in ribbon model. The crystal visible water molecules are shown a red spheres. PDB codes are the following: 4HXO (5), 4HXX (6), 4HXP (7), 4HYN (8).

providing robust interaction information of the protein–ligand complexes.

As shown in Figure 3, four fragment hits bear very different chemical moieties and yet bind to a similar position in the BRD4(I) binding site (inhibition activity data listed in Supporting Information Table S1). The [1,2,4]triazolo[4,3-*a*]pyridine ring of fragment 5 is located at the bottom of the KAc binding site, and one of the nitrogen atoms in the five-membered ring makes a hydrogen bonding interaction with the conserved residue Asn140. One of the other nitrogen atoms makes an indirect hydrogen bond with Tyr97 through a bridged water molecule. These two interactions are also observed in complex

structure of JQ1 with BRD4(I). The 3-methylisoxazole ring of fragment 5 extends to the solvent-exposed area around residue Trp81, an entrance termed the WPF shelf by Nicodeme et al.,^{11b} which is thought to be the predominant subpocket for achieving selectivity toward BET family. Among all the fragment hits, 6 is the most difficult one to precisely determine its conformation inside the binding site because hydrogen bonding interaction between BRD4(I) and this fragment is undetectable. After carefully checking the electron density map, we believe that the binding orientation of 6 presented in Figure 3 is reasonable (see Supporting Information Figure S1 for the electron density map of fragment 6). The amide group of the fragment is located in the

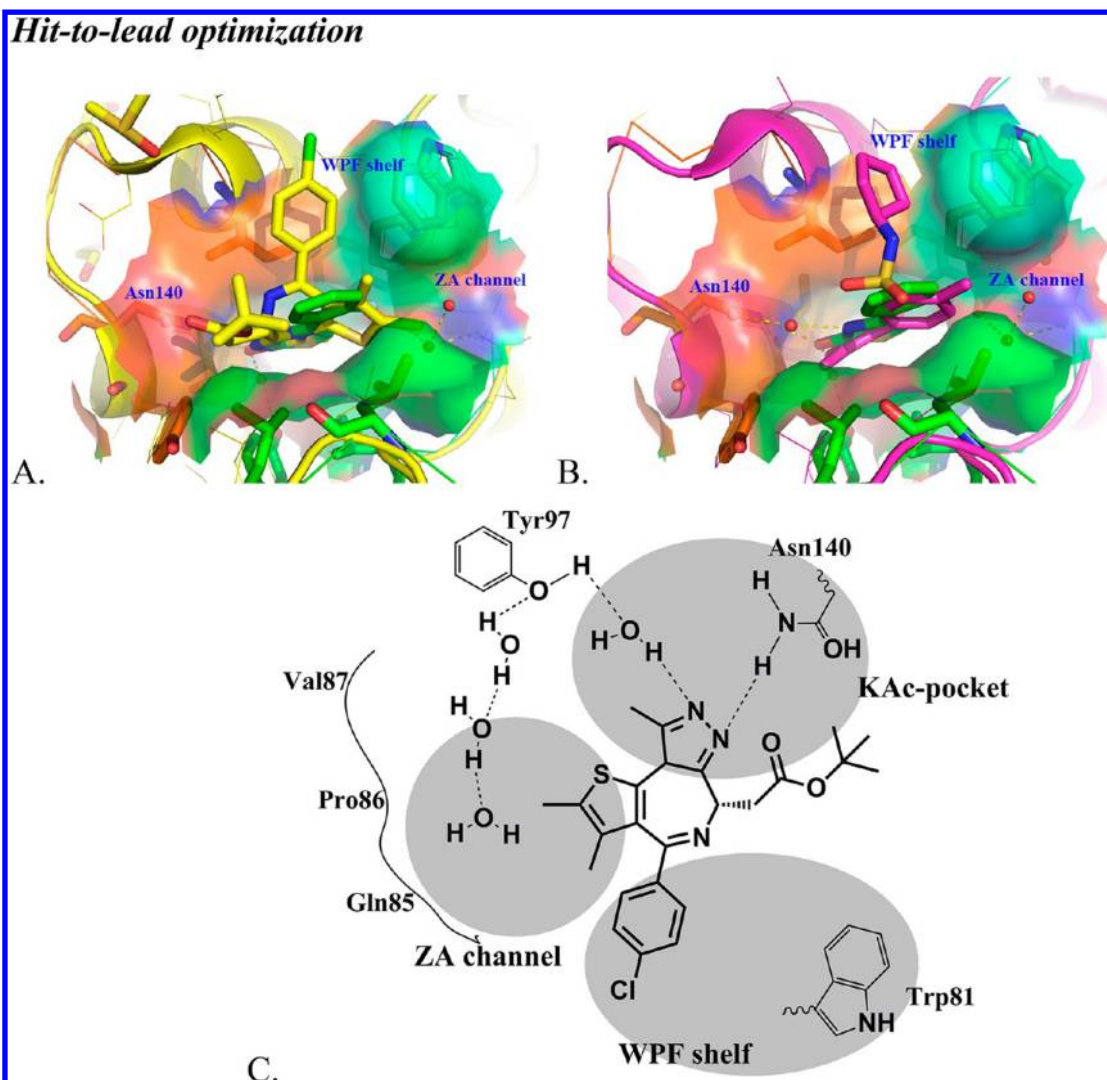


Figure 4. Superposition of crystal structures of (A) **1** (3MXF⁷) and **8** (4HXN) and (B) **4** (4A9M^{15a}) and **8** (4HXN). The ligands are shown in stick model, while the protein is shown in ribbon model. The binding site is depicted as a surface for better visualization. (C) Interaction map of JQ1 bound to BRD4(I) based on the crystal structure of 3MXF was prepared according to ref 5c.

vicinity of Asn140, but the oxygen atom to the closest atom of Asn140 is about 3.8 Å, far beyond the distance of a typical hydrogen bond. Notably, there is no visible crystallographic water molecule nearby. The fragment hit **7** utilizes the amide as a functional group to interact with the conserved residues Asn140 and Tyr97. Although the amide group is similar to the acetyl group in acetylated lysine because they both contain a carbonyl oxygen atom and a nitrogen atom, the hydrogen bonding interaction patterns between them and residues were distinct. In the crystal structure of BRD4(I) bound with the acetyl N terminal peptide of histone H3, the acetylated lysine of histone H3 forms two hydrogen bonds; one is with the nitrogen atom of amide of Asn140, and another is indirectly with Tyr97 via a water molecule. In the BRD4(I)/**7** complex, two water molecules were used as a bridge to build the hydrogen bonds between the amide group of the fragment and residue Tyr97. The fragment hit **8** also bound into the KAc pocket with a unique orientation to mimic the binding of the acetyl moiety of the native substrate. The 2-thiazolidinone core interacts with BRD4(I) by a direct hydrogen bond of its carbonyl group with the nitrogen atom of side chain of Asn140 and a water bridged hydrogen bond with Tyr97. The nitrogen atom in the 2-thiazolidinone core forms another

indirect hydrogen bond with the amide group of Asn140 through a water molecule.

Fragments **5**–**8** are diversified hits with different functional groups to interact with the vital residue Asn140 and are promising for development into novel BRD4(I) inhibitors. In the present work, we reported the exploration of the structure–activity relationship (SAR) space of fragment **8**. Optimization of other three fragments will be reported elsewhere.

Hit-to-Lead Optimization. The crystal structures of JQ1 and 3,5-dimethylisoxazole inhibitor **4** in complex with BRD4(I) were analyzed to provide the clues for optimization of the selected fragment **8**. As shown in Figure 4, the cocrystal structure reveals an excellent shape complementarity between JQ1 and BRD4(I). The key interactions are shown in Figure 4. The triazole of JQ1 forms an important hydrogen bond with the conserved residue Asn140 that contacts the acetyl acetylated lysine of histone H3K9 in the native state. There is a water mediated hydrogen bond between Tyr97 and the triazole group. This structured water is one of the four conserved water molecules situated at the bottom of the binding site. These four crystal waters together with several residues lining the ZA channel are forming a hydrogen bond network to stabilize the

BRD4(I) binding site. The thiophene moiety of JQ1 extends to the border of the ZA channel and mainly interacts with the residue Leu92 through van der Waals (VDW) interactions. Since the diazepine scaffold has a well matched bending along the surface of the binding site, the 4-chlorophenyl group can protrude out the pocket and reach the WPF shelf, forming the VDW interactions with the hydrophobic residues Trp81 and Ile146. By comparison with the crystal structures of fragment **8** and JQ1 in complex with BRD4(I) (Figure 4A), the phenyl moiety of **8** is at the top of the diazepine core, shielded by the residues Leu92 and Leu94, and the *tert*-butyl ester moiety of JQ1 is in the vicinity of the meta position of the phenyl group. The superposition of the complex structures of BRD4(I) with fragment **8** and the 3,5-dimethylisoxazole inhibitor **4** shows that the 2-thiazolidinone motif of **8** is located at the same position of 3,5-dimethylisoxazole group of **4** and forms one more water bridged hydrogen bond with the residue Asn140. The orientation of the phenyl group of fragment **8** is slightly different with the phenyl ring in compound **4**. Modification at the meta or para position of the phenyl ring of **8** may introduce further interactions with BRD4(I), as seen in the development of the 3,5-dimethylisoxazole series. Therefore, we prepared various substituents at the meta and/or para position of the phenyl moiety of **8** to identify the modifiable direction for optimization.

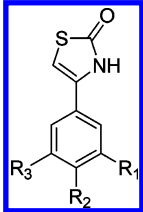
As shown in Table 1, the 3-chloro substituent of **12a** is more potent than the 3-NH₂ analogue **17**. When NH₂ was changed to

by SAR study on the series of 3,5-dimethylisoxazoles, it was found that a hydrophobic group at the WPF shelf can substantially increase the potency for BRD2(I).^{15b} As depicted in Figure 4B, the sulfonamide group can make a right angle to introduce a hydrophobic moiety toward the WPF shelf. Taking advantage of this knowledge, we synthesized some sulfonamide derivatives by varying the length and attaching aromatic groups. Moreover, to evaluate the importance of this moiety, an amide analogue and an amine analogue were also prepared for competitive binding assay.

Generally, as listed in Table 2, the sulfonamide substitution oriented at the para or meta position improves the binding affinity when comparing with compounds in Table 1, which indicates that the 2-thiazolidinone series may have similar binding modes as the 3,5-dimethylisoxazoles. As exemplified by compound **18c**, a large aromatic group attached to the sulfonamide is not tolerable at the meta position. Other substituents (**18a,b,d–f**) at meta position show similar submicromole IC₅₀ toward BRD4(I). Compared to the sulfonamide, utilizing the amide group attached to meta position of the phenyl ring (**18g**) dramatically deteriorates the binding activity to BRD4(I). A similar effect was also revealed by the inhibition activity (IC₅₀ = 22.8 μ M) of the amine substituent compound **18h**. Compound **24a** bearing a thiophene sulfonamide group at para position shows dramatically decreased inhibition for BRD4(I), while adding hydroxyl to the meta-position to **24a** to obtain **24b** can restore the activity. By scrutinizing the structures of fragment **8**, we thought the thiophene sulfonamide group at para position of compound **24b** may also extend into the WPF shelf if the sulfonamide rotates itself slightly. Clearly, **24b** or **39** containing disubstitution at the phenyl group shows good potency to BRD4(I). To rationalize further optimization, crystallization for these compounds were set up and two crystal structures of **18b** and **18d** bound to BRD4(I) were solved. As shown in Figure 5, the thiophene sulfonamide group in **18d** indeed extended to the WPF shelf and made VDW interactions with the subpocket lining by the residues Trp81 and Ile146. Surprisingly, the binding position of **18b** is distinct from the **18d** by its phenylmethane sulfonamide group entering the ZA channel, where it rotates the sulfonamide group down to form a hydrogen bonding network. As its crystal structure shows, the two oxygen atoms of the sulfonamide group make two hydrogen bonds with a water molecule, and one oxygen further forms a hydrogen bond with the side chain of the residue Gln85. Another oxygen atom contacts a second water molecule, which further forms two hydrogen bonds with the backbone of Pro86 and Asp88. Although the extensive hydrogen bonds were formed around that position, the binding activity did not surpass that of **18d**. Nevertheless, this subpocket, which was undescribed in previous studies on bromodomain, still provides a new direction for optimization.

On the basis of this round of optimization, it was found that the meta position of the phenyl ring of fragment **8** can make different interactions with the binding site of BRD4(I). The crystal structures show that the sulfonamide group of **18b** is no longer needed to make the right-angle turn to interact with BRD4(I) as in **18d**. We speculate that the sulfonamide group in **18b** is not a critical component for binding and can be substituted with its bioisostere amide group, since the amide group can fulfill the interactions with crystal water and stabilize the linear conformation of the phenylmethane group. Besides, the two different binding conformations encourage us to take the approach to merge these binding motifs to increase the binding

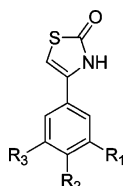
Table 1. Effects of Substituents of 2-Thiazolidinones on Inhibition of BRD4(I) from Fluorescence Anisotropy Assay^a

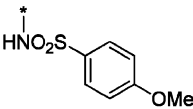
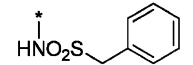
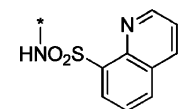
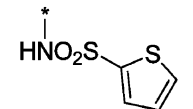
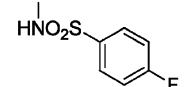
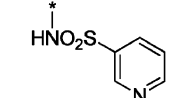
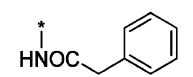
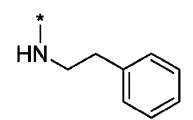
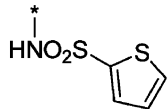
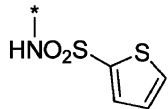
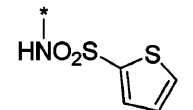


compd	R ₁	R ₂	R ₃	BRD4(I) IC ₅₀ (μ M)
12a	Cl	H	H	24.0 \pm 1.8
17	NH ₂	H	H	42.0 \pm 0.4
23a	H	NH ₂	H	51.0 \pm 3.0
23b	OH	NH ₂	H	23.8 \pm 2.7
38	NH ₂	H	NH ₂	50.7 \pm 18.1

^aPositive control compound **4** has an IC₅₀ of 0.8 \pm 0.1 μ M. The IC₅₀ in the table was calculated from two independent experimental measurements. The fluorescence compound used in the assay is JQ1-FITC. (JQ1 has an IC₅₀ of 58.7 \pm 8.7 nM in the current FA assay system. The chemical structure of JQ1 linked with fluorescein isothiocyanate and the synthesis route are provided in Supporting Information Scheme S1.)

para position to afford **23a**, it was slightly less potent than **17**. The 4-amino-3-hydroxyl disubstituted analogue **23b** is the most potent fragment in Table 1, indicating that adding a hydroxyl group at the meta position of phenyl can improve ligand binding. The IC₅₀ of **38**, containing 3,5-diamino substituent, is about 50 μ M. By comparison with **17**, it did not show improvement by the additional amine group. The differences in binding affinities may due to the solvation effect based on the fact that there is no residue in the vicinity of the ligand as revealed by the cocrystal structure of fragment **8**. Through synthesis and enzymatic inhibition assay of these analogues of fragment **8**, the utility of this identified fragment hit is further strengthened. As suggested

Table 2. Effects of Substituents of 2-Thiazolidinones on Inhibition of BRD4(I) from Fluorescence Anisotropy Assay^a


Compound	R ₁	R ₂	R ₃	BRD4(I) IC ₅₀ (μM)
18a		H	H	4.4±0.2
18b		H	H	4.1±0.4
18c		H	H	45.7% ^b @50μM ^b 54.7% ^b @50μM
18d		H	H	4.1±0.5
18e		H	H	3.70±0.7
18f		H	H	10.0±0.1
18g		H	H	45.6% ^b @50μM ^b 48.6% ^b @50μM
18h		H	H	22.8±3.2
24a	H		H	41.9% ^b @50μM ^b 38.6% ^b @50μM
24b	OH		H	3.3±0.5
39		H	NH ₂	2.6±0.1

^aThe IC₅₀ was calculated from two independent experimental measurements. ^bThe value is BRD4(I) inhibition ratio at a ligand concentration of 50 μM measured with the fluorescence anisotropy method.

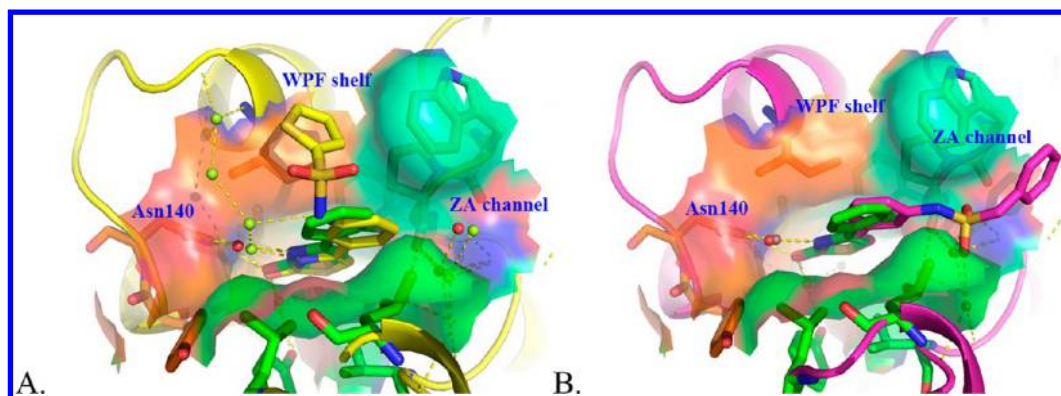


Figure 5. Superposition of cocystal structure fragment 8 with cocystal structures of compounds **18b** and **18d** (PDB codes 4HXS (**18b**) and 4HXR (**18d**)). The ligands are shown in stick model, while the protein is shown in ribbon model. The binding site is depicted as a surface for better visualization.

affinity. Therefore, second round optimization was conducted for this series using these hypotheses anticipating further increases to the binding affinity to the target domain.

As listed in Table 3, adding the amide groups to meta position improves the binding affinity compared with compound **24a**. For compounds such as **33a–d**, they bound to BRD4(I) with IC_{50} values lower than $5 \mu\text{M}$, which is at least 10-fold more potent than compound **24a**. If the amide substituent is maintained at meta position, the compounds (**33a–e**) with thiophene sulfonamide substituted at para position would be less potent than the compounds (**40a–d**) that bear thiophene sulfonamide at another meta position. **40a** was identified as the most active compound **40a** and is 17-fold potent than compound **18d** that bears only one thiophene sulfonamide at the meta position of the phenyl ring.

To verify the hypotheses about the binding mode, we crystallized two compounds **40b** and **40d** with BRD4(I) and solved the structures. As shown in Figure 6, the inhibitors bound to the BRD4(I) as expected, the sulfonamide group turning the thiophene group to the WPF shelf, while the amide group extends into the ZA channel and makes extensive hydrogen bonding interactions with residues lining the ZA channel. This unique binding conformation suggests that the ZA channel constitutes an additional subpocket to those previously described and can be utilized to improve the inhibitor binding.

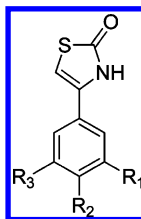
In Vitro PK Assessment. There is growing evidence that early assessment of in vitro DMPK profiles of lead compounds can reduce the attrition rate often encountered in drug development.²⁹ To better validate the usefulness of the 2-thiazolidinone scaffold as the BRD4(I) inhibitors, we selected **18d** and **40a** as the representatives from first round and second round optimizations to perform a PK study in vitro. Compound **40a** differs from **18d** by containing an extra thiophene amide at meta position of benzene group. Although DMPK studies in vitro on these two compounds cannot be projected to the whole series, the test may provide the clues of metabolic stability issues related to the important functional groups including the 2-thiazolidinone core, thiophene sulfonamide, and thiophene amide. As shown in Table 4, the results showed that **18d** and **40a** have very clean metabolic stability profiles. The liver microsome assays indicated that **18d** and **40a** were relatively stable in human or mice liver microsomes, and only compound **18d** showed slightly high clearance rate of about $120 \mu\text{L min}^{-1} \text{mg}^{-1}$ in mice liver microsomes. In addition to this, several cytochrome P450 enzymes commonly metabolizing exogenous

chemicals were used to test the direct inhibition of **18d** and **40a**. The evaluations showed that two compounds inhibited the CYPs at less than 50% ratios at $10 \mu\text{M}$, which reinforced the metabolic stability of these compounds. Therefore, from the PK profiling in vitro, it demonstrated the value of the 2-thiazolidinone series as a novel scaffold and the potential for developing into useful inhibitors of BRD4(I).

Cellular Activity. To complete the lead druglike profile of 2-thiazolidinones, we performed cellular activity assays, including the cancer cell proliferation inhibition and target related c-myc mRNA quantitative real time-PCR (RT-qPCR) test. Initially, we screened against common cancer cells to identify the sensitive cell lines related to BRD4 and found that the HT-29 cell line is sensitive to BRD4 inhibitor JQ1. The results showed that JQ1 inhibits HT-29 cell with a GI_{50} of about $2.3 \pm 1.6 \mu\text{M}$ and 50% c-myc mRNA inhibition ratio at $0.36 \mu\text{M}$. Then 13 compounds with good enzymatic inhibition potency were selected to investigate the cellular effects. As shown in Figure 7, the cellular proliferation inhibition values are not well correlated with the enzymatic inhibition potencies, especially for the disubstituted compounds **40a–d**. This phenomenon was revealed by several statistical analyses of the correlation of ADME properties with physicochemical properties of compounds.³⁰ From a physicochemical property point of view, the compounds with low molecular weight and low calculated log P , such as **39**, are clearly more potent in cells, which indicated that large molecules such as **33d** may have issues involving poor membrane permeability. Specifically, the calculated log P of **39** is 1.27, while **33d** has log P of 3.65. The calculated polar surface areas (PSA) of these two compounds are not distinguishable (101.3 versus 104.4), which may indicate that the PSA plays a less important role in the cellular effects of this series. Compared with the 3,5-dimethylisoxazole compound **4** ($GI_{50} = 22.5 \pm 6.1 \mu\text{M}$), compound **39** has a slightly weak inhibition to HT-29 cells with a GI_{50} of about $37.3 \pm 15.5 \mu\text{M}$. The other two compounds **18e** and **33d** are less potent with GI_{50} of about 47.8 and $63.6 \mu\text{M}$. This HT-29 cell proliferation assay coincides well with the effects of these compounds on c-myc mRNA expression (shown in Figure 8), with compounds **4** and **39** having more than 50% inhibition. These data implied that the 2-thiazolidinones inhibited the HT-29 cells through the BRD4 dependent pathway.

CONCLUSION

In summary, with the aim of identifying novel chemotypes as bromodomain inhibitors, we adopted a fragment-based drug

Table 3. Effects of Substituents of 2-Thiazolidinones on Inhibition of BRD4(I) from Fluorescence Anisotropy Assay^a

Compound number	R ₁	R ₂	R ₃	BRD4(I) IC ₅₀ (μM)
33a			H	3.5±1.0
33b			H	2.6±0.2
33c			H	2.4±0.6
33d			H	2.5±0.2
33e			H	25.7% ^b @50μM 20.2% ^b @50μM
40a		H		0.23±0.04
40b		H		2.2±0.1
40c		H		0.57±0.1
40d		H		0.79±0.8

^aThe IC₅₀ was calculated from two independent experiment measurements. ^bThe value is BRD4(I) inhibition ratio at a ligand concentration of 50 μM measured with the fluorescence anisotropy method.

discovery approach to screen our fragment library, which consisted of about 500 small molecular weight fragments. After the refinement of the fragment library using computational docking methods, 41 fragments that fulfill conserved hydrogen

bonding interactions with the Asn140 in BRD4(I) binding site were cherry-picked and were further interrogated using X-ray crystallographic diffraction methods. These can allow simultaneously visualization of the binding modes. In total more than 60

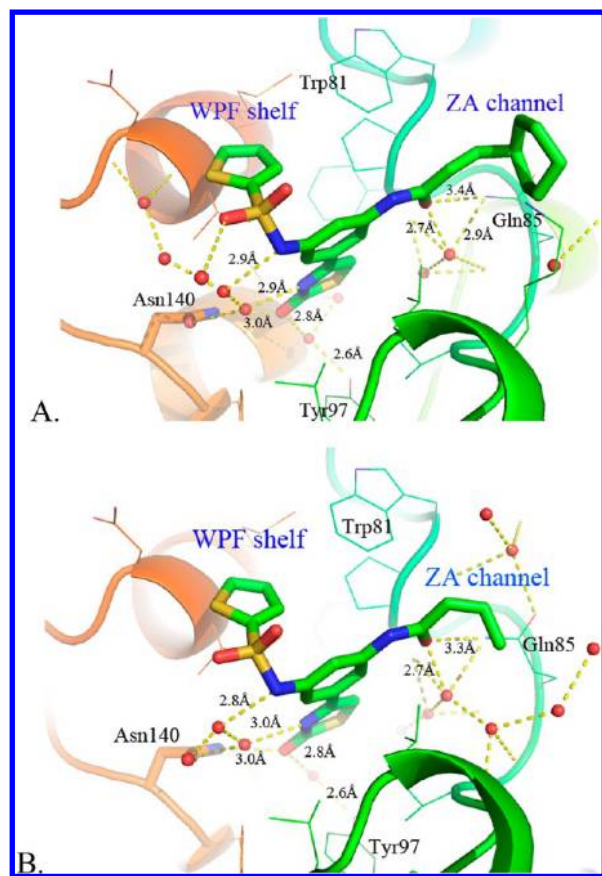


Figure 6. Cocystal structures of BRD4(I) with **40b** and **40d** (PDB codes 4HXL (**40b**) and 4HXM (**40d**)). The ligands are shown in stick model, while the protein is shown as a ribbon.

crystals were diffracted and the structures solved. Among them, 4 crystal structures have sufficient strong electron density in BRD4(I) binding sites, and corresponding fragments were allowing interrogation of binding conformations. The fragment that bears a 2-thiazolidinone core was carried through an optimization cycle to explore the structure–activity relationships. On the basis of structure guided medicinal chemistry modification, we identified some compounds of this series that process potent inhibition of about 0.3 μM toward BRD4(I). The PK study in vitro and cellular activity assays further demonstrated that the 2-thiazolidinone is an interesting scaffold, which is both druggable and has potential to be developed into inhibitors that antagonize acetylsine–bromodomain interactions.

EXPERIMENTAL SECTION

Chemistry. General. ^1H NMR (400 MHz) spectra were recorded by using a Varian Mercury-400 high performance digital FT-NMR spectrometer with tetramethylsilane (TMS) as an internal standard. ^{13}C NMR (100 or 125 MHz) spectra were recorded by using a Varian Mercury-400 high performance digital FT-NMR spectrometer or Varian Mercury-500 high performance digital FT-NMR spectrometer. Abbreviations for peak patterns in NMR spectra are the following: br

= broad, s = singlet, d = doublet, and m = multiplet. Low-resolution mass spectra were obtained with a Finnigan LCQ Deca XP mass spectrometer using a CAPCELL PAK C18 (50 mm \times 2.0 mm, 5 μm) or an Agilent ZORBAX Eclipse XDB C18 (50 mm \times 2.1 mm, 5 μm) in positive or negative electrospray mode. High-resolution mass spectra were recorded by using a Finnigan MAT-95 mass spectrometer or an Agilent Technologies 6224 TOF mass spectrometer. Purity of all compounds was determined by analytical Gilson high-performance liquid chromatography (HPLC) using a YMC ODS3 column (50 mm \times 4.6 mm, 5 μm). Conditions were as follows: $\text{CH}_3\text{CN}/\text{H}_2\text{O}$ eluent at 2.5 mL min^{-1} flow [containing 0.1% trifluoroacetic acid (TFA)] at 35 $^\circ\text{C}$, 8 min, gradient 5% CH_3CN to 95% CH_3CN , monitoring by UV absorption at 214 and 254 nm. TLC analysis was carried out with glass precoated silica gel GF254 plates. TLC spots were visualized under UV light. Flash column chromatography was performed with a Teledyne ISCO CombiFlash R_f system. All solvents and reagents were used directly as obtained commercially unless otherwise noted. Anhydrous dimethylformamide was purchased from Acros and was used without further drying. All air and moisture sensitive reactions were carried out under an atmosphere of dry argon with heat-dried glassware and standard syringe techniques. Microwave reactions were performed with a Biotage Initiator focused beam microwave reactor (400 W). Melting points were determined using a SGW X-4 hot stage microscope and are uncorrected.

Synthetic Procedures. Compounds **9**, **13**, **19b**, **20a**, **25**, and **34** were purchased. Other compounds were prepared by one of five schemes. Treatment of different acetophenones with CuBr_2 gave the desired 2-bromoacetophenones. KSCN was added to obtain the crude 2-thiocyanatoethanone products which were used without further purification. The thiazol-2(3H)-one products were obtained by addition of acetic acid and 50% H_2SO_4 with heating to 100 $^\circ\text{C}$ for 1 h. Nitro reduction was achieved through iron and ammonium chloride. The sulfonamide products were prepared from aminophenylthiazol-2(3H)-one and commercially available sulfonyl chlorides.

Procedure 1a of Scheme 1. To a solution of 1-(3-chlorophenyl)ethanone **9** (200 mg, 1.294 mmol) in EtOAc (20 mL) was added CuBr_2 (347 mg, 1.552 mmol), and the mixture was heated to reflux overnight. The mixture was cooled to room temperature and extracted with EtOAc (3 \times 20 mL). The combined organic layers were washed with brine (30 mL), dried (Na_2SO_4), filtered, and concentrated in vacuo to give the crude product. Purification by silica gel column chromatography (gradient elution, gradient 5–20% EtOAc/petroleum ether) gave 2-bromo-1-(3-chlorophenyl)ethanone **10** as a colorless solid (220 mg, 0.942 mmol, 72.8% yield). ^1H NMR (400 MHz, CDCl_3) δ 7.96 (t, J = 1.9 Hz, 1H), 7.86 (m, 1H), 7.59 (m, 1H), 7.45 (t, J = 7.9 Hz, 1H), 4.43 (s, 2H).

Procedure 1b of Scheme 1. To a suspension of KSCN (166 mg, 1.713 mmol) in acetone (10 mL) was added **10** (100 mg, 0.428 mmol), and the mixture was stirred at room temperature for 30 min. The mixture was concentrated in vacuo to give the crude product **11** which was used for the next step without further purification.

Procedure 1c of Scheme 1. To a suspension of the crude product **11** in acetic acid (5 mL) was added 50% H_2SO_4 (0.5 mL), and the mixture was heated to 100 $^\circ\text{C}$ for 1 h. The mixture was poured into ice–water. The product was precipitated and collected by filtration. The filtrate was concentrated in vacuo, suspended in MeOH (5 mL), and collected by filtration. The combined solid was dried in vacuo to give 4-(3-chlorophenyl)thiazol-2(3H)-one **12** as a powdery colorless solid (62 mg, 0.293 mmol, 68.4% yield). Mp 146–148 $^\circ\text{C}$; ^1H NMR (400 MHz, DMSO) δ 11.85 (s, 1H), 7.78 (t, J = 1.8 Hz, 1H), 7.64 (dt, J = 7.5, 1.5 Hz, 1H), 7.46 (t, J = 7.7 Hz, 1H), 7.42 (m, 1H), 7.00 (d, J = 1.6 Hz, 1H); ^{13}C

Table 4. In Vitro Liver Microsome Stability Assay and Cytochrome P450 Enzymes Inhibition Assay

compd	HLM CL_{inv} $\mu\text{L min}^{-1} \text{mg}^{-1}$	MLM CL_{inv} $\mu\text{L min}^{-1} \text{mg}^{-1}$	CYP inhibition ratio, % (compd concn of 10 μM)				
			3A4	2D6	2C9	1A2	2C19
18d	24	120	17	22	34	16	36
40a	18	52	8	20	41	29	39

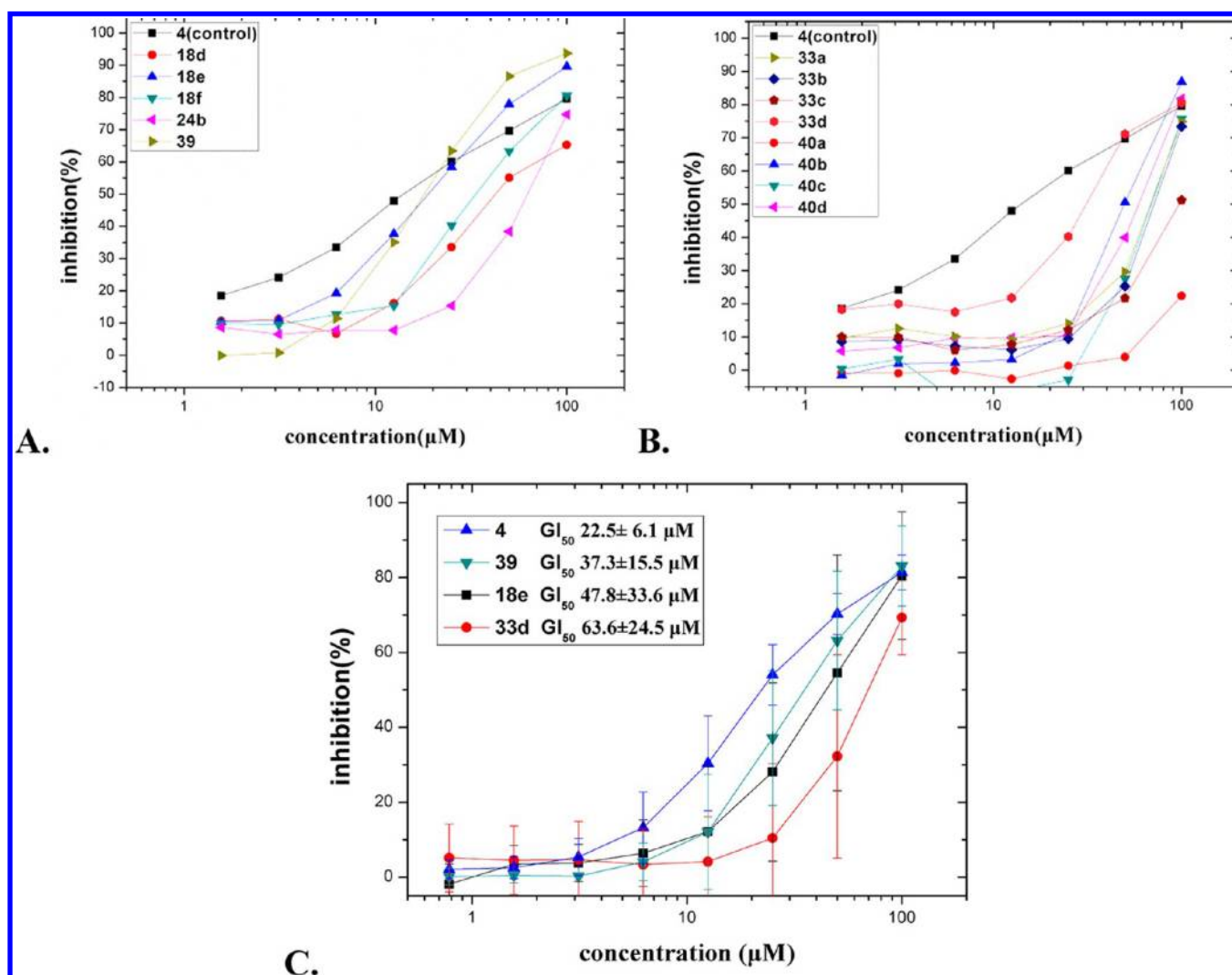


Figure 7. Proliferation inhibition of compounds in human colon cancer HT-29 cells. The cells were treated with gradient concentrations of the tested compounds for 72 h followed by SRB assays. Parts A and B show the inhibition profile of 13 selected compounds. (C) Three compounds that showed better inhibition as well as the positive control compound 4 were further studied to calculate GI_{50} values (from four independent experiments and represented as the mean \pm SD).

NMR (126 MHz, DMSO) δ 173.18, 134.20, 132.84, 131.99, 131.18, 128.73, 125.08, 123.91, 100.50; HRMS m/z (ESI) found $[M + H]^+$ 211.9942, $C_9H_7^{35}ClNOS^+$ requires 211.9937; LCMS m/z (ESI) found $[M + H]^+$ 212.1. Retention time of 2.97 min, >99% pure.

Procedure 2a of Scheme 2. To a solution of 1-(3-nitrophenyl)ethanone **13** (1g, 6.06 mmol) in EtOAc (50 mL) was added $CuBr_2$ (1.623 g, 7.27 mmol), and the mixture was heated to reflux overnight. The mixture was cooled to room temperature and extracted with EtOAc (3 \times 50 mL). The combined organic layers were washed with brine (50 mL), dried (Na_2SO_4), filtered, and concentrated in vacuo to give the crude product. Purification by silica gel column chromatography (gradient elution, gradient 5–20% EtOAc/petroleum ether) gave 2-bromo-1-(3-nitrophenyl)ethanone **14** as a yellow solid (1.13g, 76% yield). 1H NMR (400 MHz, $CDCl_3$) δ 8.81 (t, J = 2.0 Hz, 1H), 8.48 (m, 1H), 8.35 (dd, J = 7.8, 1.6 Hz, 1H), 7.77 (dd, J = 11.9, 4.1 Hz, 1H), 4.53 (s, 2H).

Procedure 2b of Scheme 2. To a suspension of KSCN (1.114g, 11.47 mmol) in acetone (20 mL) was added **14** (700 mg, 2.87 mmol), and the mixture was stirred at room temperature for 30 min. The mixture was concentrated in vacuo to give the crude product **15** which was used for the next step without further purification.

Procedure 2c of Scheme 2. To a suspension of the crude product **15** in acetic acid (10 mL) was added 50% H_2SO_4 (1 mL), and the mixture was heated to 100 $^\circ C$ for 1 h. The mixture was poured into ice–water.

The product was precipitated and collected by filtration. The filtrate was concentrated in vacuo, suspended in MeOH (10 mL), and collected by filtration. The solid was dried in vacuo to give 4-(3-nitrophenyl)thiazol-2(3H)-one **16** as a yellow solid (510 mg, 80% yield). 1H NMR (400 MHz, DMSO) δ 12.09 (s, 1H), 8.53 (t, J = 1.8 Hz, 1H), 8.21 (dd, J = 8.2, 2.2 Hz, 1H), 8.11 (d, J = 8.1 Hz, 1H), 7.74 (t, J = 8.1 Hz, 1H), 7.15 (s, 1H); LCMS m/z (ESI, negative) found $[M - H]$ 221.1. Retention time of 2.66 min, >99% pure.

Procedure 2d of Scheme 2. To a solution of **16** (1.05g, 4.73 mmol) in EtOH (10 mL) was added fine Fe powder (1.319 g, 23.6 mmol) at 50–55 $^\circ C$ followed by NH_4Cl solution (1.26 g, 23.6 mmol in 2 mL water). The reaction mixture was refluxed for 1 h, and EtOH was removed from the reaction mixture under reduced pressure. The residue was basified with $NaHCO_3$ solution (pH 7–8) and extracted with EtOAc (3 \times 50 mL). The combined organic extracts were washed with brine, dried (Na_2SO_4), and concentrated under reduced pressure. Purification by silica gel column chromatography (gradient elution, gradient 0–5% MeOH/ CH_2Cl_2) gave 4-(3-aminophenyl)thiazol-2(3H)-one **17** as a yellow solid (0.7g, 77% yield). Mp 182–183 $^\circ C$; 1H NMR (400 MHz, DMSO) δ 11.62 (s, 1H), 7.05 (t, J = 7.7 Hz, 1H), 6.78–6.73 (m, 2H), 6.57 (ddd, J = 8.0, 2.2, 1.0 Hz, 1H), 6.53 (d, J = 1.6 Hz, 1H), 5.21 (s, 2H); ^{13}C NMR (126 MHz, DMSO) δ 173.42, 149.36, 135.31, 130.87, 129.77, 114.91, 113.26, 110.55, 97.36; HRMS m/z (ESI)

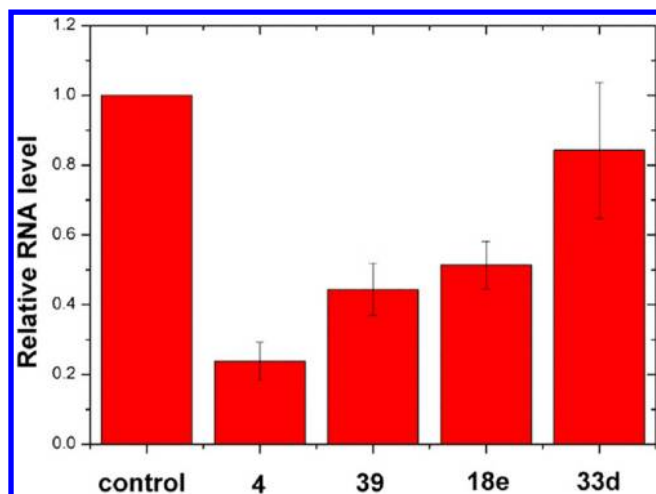


Figure 8. Inhibition of compounds on the expression of c-myc mRNA. HT-29 cells were treated with compounds (10 μ M) for 24 h. Total RNA was isolated and reverse-transcribed for RT-qPCR analyses. The data were expressed as the mean \pm SD, representing the relative levels of c-myc mRNA from three independent experiments.

found $[M + H]^+$ 193.0546, $C_9H_{10}N_2OS^+$ requires 193.0436; LCMS m/z (ESI) found $[M + H]^+$ 193.1. Retention time of 1.58 min, >98% pure.

Procedure 2e of Scheme 2. To a solution of 17 (100 mg, 0.520 mmol) in a mixture (1:1) of CH_2Cl_2 (3 mL) and pyridine (3 mL) was added 4-methoxybenzene-1-sulfonyl chloride (129 mg, 0.624 mmol) at room temperature under a nitrogen atmosphere. The resulting mixture was allowed to stir for 2 h. Upon completion of the reaction, the crude mixture was diluted with CH_2Cl_2 and washed with water followed by 1 N HCl (20 mL). The resulting organic layer was then dried over Na_2SO_4 and concentrated under reduced pressure. Purification by silica gel column chromatography (gradient elution, gradient 0–5% MeOH/ CH_2Cl_2) gave 4-methoxy-*N*-(3-(2-oxo-2,3-dihydrothiazol-4-yl)phenyl)benzenesulfonamide 18a (120 mg, 0.331 mmol, 63.7% yield). Mp 86–88 $^{\circ}C$; 1H NMR (400 MHz, DMSO) δ 11.81 (s, 1H), 10.32 (s, 1H), 7.74 (d, J = 8.9 Hz, 2H), 7.37 (s, 1H), 7.27 (m, 2H), 7.05 (m, 3H), 6.62 (s, 1H), 3.79 (s, 3H); ^{13}C NMR (101 MHz, DMSO) δ 173.32, 162.86, 138.89, 133.95, 131.29, 131.05, 130.13, 129.34, 121.14, 120.31, 116.73, 114.81, 99.16, 56.01; HRMS m/z (ESI) found $[M + H]^+$ 363.0474, $C_{16}H_{15}N_2O_4S_2^+$ requires 363.0473; LCMS m/z (ESI) found $[M + H]^+$ 363.1. Retention time of 2.94 min, >99% pure.

Compounds 18b–f were prepared according to the general procedure 2e.

***N*-(3-(2-Oxo-2,3-dihydrothiazol-4-yl)phenyl)-1-phenylmethanesulfonamide 18b.** Mp 175–177 $^{\circ}C$; 1H NMR (400 MHz, DMSO) δ 11.89 (s, 1H), 9.98 (s, 1H), 7.41–7.26 (m, 8H), 7.11 (m, 1H), 6.68 (d, J = 1.9 Hz, 1H), 4.58 (s, 2H); ^{13}C NMR (126 MHz, DMSO) δ 173.49, 139.49, 134.26, 131.41, 131.31, 130.30, 130.00, 128.86, 128.70, 120.71, 119.93, 115.60, 99.24, 57.68; HRMS m/z (ESI) found $[M + H]^+$ 347.0525, $C_{16}H_{15}N_2O_3S_2^+$ requires 347.0524; LCMS m/z (ESI) found $[M + H]^+$ 347.0. Retention time of 2.93 min, >92% pure.

***N*-(3-(2-Oxo-2,3-dihydrothiazol-4-yl)phenyl)quinoline-8-sulfonamide 18c.** Mp 262–263 $^{\circ}C$; 1H NMR (400 MHz, DMSO) δ 11.73 (s, 1H), 10.24 (s, 1H), 9.16 (dd, J = 4.2, 1.8 Hz, 1H), 8.52 (dd, J = 8.0, 1.8 Hz, 1H), 8.42 (dd, J = 7.4, 1.4 Hz, 1H), 8.27 (dd, J = 8.3, 1.4 Hz, 1H), 7.72 (m, 2H), 7.38 (s, 1H), 7.17–7.09 (m, 2H), 6.91 (m, 1H), 6.48 (d, J = 1.3 Hz, 1H); ^{13}C NMR (126 MHz, DMSO) δ 173.30, 151.97, 143.09, 138.80, 137.47, 135.45, 134.81, 133.99, 132.64, 130.80, 129.84, 128.84, 126.12, 123.12, 121.01, 120.39, 116.72, 98.91; HRMS m/z (ESI) found $[M + H]^+$ 384.0518, $C_{18}H_{14}N_3O_3S_2^+$ requires 384.0477; LCMS m/z (ESI) found $[M + H]^+$ 384.1. Retention time of 2.96 min, >96% pure.

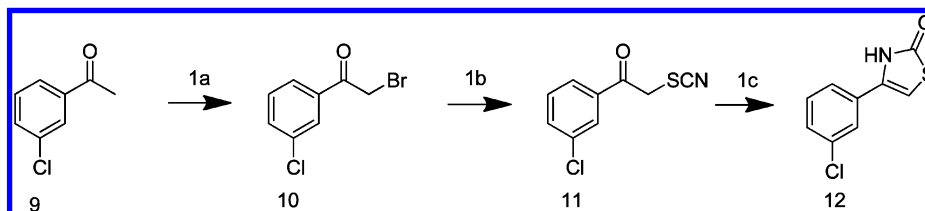
***N*-(3-(2-Oxo-2,3-dihydrothiazol-4-yl)phenyl)thiophene-2-sulfonamide 18d.** Mp 231–233 $^{\circ}C$; 1H NMR (400 MHz, DMSO) δ 11.82 (s, 1H), 10.56 (s, 1H), 7.90 (dd, J = 5.0, 1.4 Hz, 1H), 7.59 (dd, J = 3.8, 1.4 Hz, 1H), 7.40 (d, J = 1.1 Hz, 1H), 7.35–7.30 (m, 2H), 7.12 (dd, J = 5.0, 3.8 Hz, 1H), 7.09 (m, 1H), 6.64 (d, J = 1.6 Hz, 1H); ^{13}C NMR (126 MHz, DMSO) δ 173.34, 140.17, 138.45, 133.98, 133.93, 133.09, 131.15, 130.23, 128.12, 121.77, 120.98, 117.39, 99.30; HRMS m/z (ESI) found $[M + H]^+$ 338.9949, $C_{13}H_{11}N_2O_3S_3^+$ requires 338.9932; LCMS m/z (ESI) found $[M + H]^+$ 339.1. Retention time of 2.77 min, >98% pure.

4-Fluoro-*N*-(3-(2-oxo-2,3-dihydrothiazol-4-yl)phenyl)benzenesulfonamide 18e. Mp 201–202 $^{\circ}C$; 1H NMR (400 MHz, DMSO) δ 11.81 (s, 1H), 10.46 (s, 1H), 7.84 (m, 2H), 7.44–7.35 (m, 3H), 7.29 (d, J = 6.3 Hz, 2H), 7.02 (m, 1H), 6.64 (s, 1H); ^{13}C NMR (126 MHz, DMSO) δ 173.36 (s), 165.80, 163.80, 138.52, 136.14, 133.91, 131.21, 130.29, 130.21, 121.66, 120.88, 117.37, 117.07, 116.89, 99.35; HRMS m/z (ESI) found $[M + H]^+$ 351.0275, $C_{15}H_{12}FNO_3S_2^+$ requires 351.0273; LCMS m/z (ESI) found $[M + H]^+$ 351.1. Retention time of 2.94 min, >94% pure.

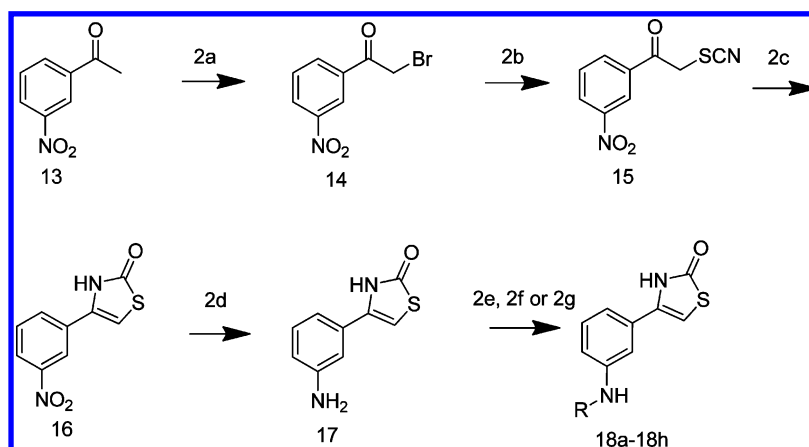
***N*-(3-(2-Oxo-2,3-dihydrothiazol-4-yl)phenyl)pyridine-3-sulfonamide 18f.** Mp 227–229 $^{\circ}C$; 1H NMR (400 MHz, DMSO) δ 11.82 (s, 1H), 10.64 (s, 1H), 8.91 (d, J = 2.3 Hz, 1H), 8.79 (d, J = 4.9 Hz, 1H), 8.14 (d, J = 8.0 Hz, 1H), 7.61 (dd, J = 8.1, 5.0 Hz, 1H), 7.38 (s, 1H), 7.36–7.26 (m, 2H), 7.05 (d, J = 7.3 Hz, 1H), 6.67 (s, 1H); ^{13}C NMR (101 MHz, DMSO) δ 173.30, 154.01, 147.49, 138.02, 136.03, 135.17, 133.72, 131.23, 130.35, 124.81, 121.96, 121.14, 117.64, 99.48; HRMS m/z (ESI) found $[M + H]^+$ 334.0332, $C_{14}H_{12}N_3O_3S_2^+$ requires 334.0320; LCMS m/z (ESI) found $[M + H]^+$ 334.1. Retention time of 2.48 min, >97% pure.

Procedure 2f of Scheme 2. To a solution of 17 (120 mg, 0.624 mmol) in anhydrous DMF (3 mL) at 0 $^{\circ}C$ was added DIPEA (0.496 mL, 2.84 mmol). After 10 min TBTU (364 mg, 1.135 mmol) was added and the resulting mixture stirred at the same temperature for 30 min. 2-Phenylacetic acid (77 mg, 0.567 mmol) was added. The resulting mixture was stirred at room temperature for 6 h. The mixture was extracted with EtOAc (50 mL), washed with brine, dried (Na_2SO_4), and concentrated in vacuo. The crude was purified by flash chromatography on silica gel (gradient elution, gradient 0–5% MeOH/ CH_2Cl_2) to give *N*-(3-(2-oxo-2,3-dihydrothiazol-4-yl)phenyl)-2-phenylacetamide 18g (95 mg, 0.306 mmol, 53.9% yield). Mp 247–249 $^{\circ}C$; 1H NMR (400 MHz, DMSO) δ 11.77 (s, 1H), 10.28 (s, 1H), 7.88 (s, 1H), 7.53 (d, J = 8.0 Hz, 1H), 7.42–7.16 (m, 7H), 6.63 (s, 1H), 3.66 (s, 2H); ^{13}C NMR (101 MHz, DMSO) δ 173.35, 169.70, 139.98, 136.23, 134.42, 130.71, 129.71, 129.54, 128.71, 126.98, 120.58, 119.97, 116.26, 98.69, 43.68; HRMS m/z (ESI) found $[M + Na]^+$ 333.0693, $C_{17}H_{14}N_2O_2NaS^+$

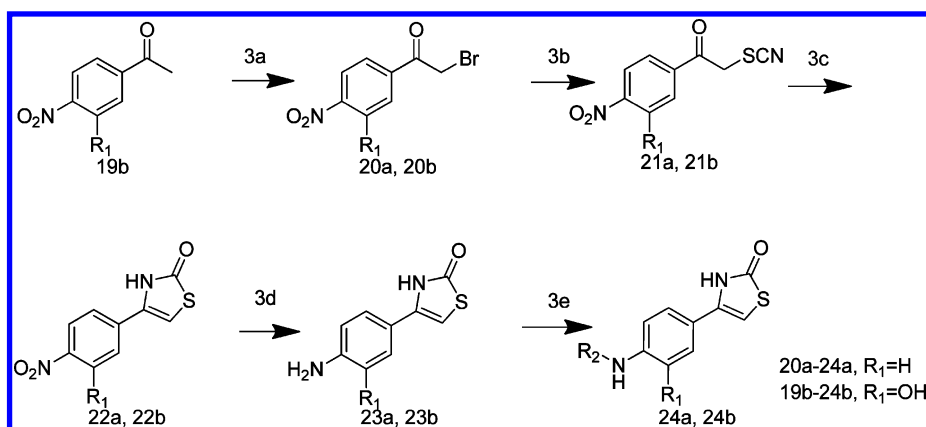
Scheme 1^a



^aReagents and conditions: (1a) $CuBr_2$, EtOAc, 80 $^{\circ}C$; (1b) KSCN, acetone, rt; (1c) 50% H_2SO_4 , acetic acid, 100 $^{\circ}C$.

Scheme 2^a

^aReagents and conditions: (2a) CuBr₂, EtOAc, 80 °C; (2b) KSCN, acetone, rt; (2c) 50% H₂SO₄, acetic acid, 100 °C; (2d) Fe, NH₄Cl, EtOH, 80 °C; (2e) R₂SO₂Cl, CH₂Cl₂, pyridine, rt; (2f) R₂COCl, DIPEA, TBTU, DMF, rt; (2g) R₂Br, Pd₂(dba)₃, Cs₂CO₃, X-phos, DMF, 100 °C.

Scheme 3^a

^aReagents and conditions: (3a) CuBr₂, EtOAc, 80 °C; (3b) KSCN, acetone, rt; (3c) 50% H₂SO₄, acetic acid, 100 °C; (3d) Fe, NH₄Cl, EtOH, 80 °C; (3e) R₂SO₂Cl, CH₂Cl₂, pyridine, rt.

requires 333.0674; LCMS *m/z* (ESI) found [M + H]⁺ 311.1. Retention time of 2.90 min, >99% pure.

Procedure 2g of Scheme 2. To a dry 10–20 mL microwave vial were added 17 (120 mg, 0.624 mmol), (2-bromoethyl)benzene (0.085 mL, 0.624 mmol), X-phos (11.90 mg, 0.025 mmol), Pd₂dba₃ (11.43 mg, 0.012 mmol), and Cs₂CO₃ (407 mg, 1.248 mmol) in DMF (3 mL) under a nitrogen atmosphere. The vial was sealed and heated in a microwave reactor at 120 °C for 1 h. The mixture was extracted with EtOAc (3 × 20 mL). The combined organic layers were washed with brine and dried (Na₂SO₄). The solvent was evaporated and purified by flash chromatography (gradient elution, gradient 0–5% MeOH/CH₂Cl₂) to afford the desired product 4-(3-(phenethylamino)phenyl)-thiazol-2(3H)-one **18h** as a solid (91 mg, 0.307 mmol, 49.2% yield). Mp 99–101 °C; ¹H NMR (400 MHz, DMSO) δ 7.25–7.16 (m, 3H), 7.11 (t, *J* = 7.8 Hz, 1H), 6.95 (d, *J* = 6.6 Hz, 2H), 6.67 (m, 1H), 6.55 (s, 1H), 6.47 (d, *J* = 7.5 Hz, 1H), 6.31 (s, 1H), 5.32 (s, 2H), 3.83 (t, *J* = 8.1 Hz, 2H), 2.68 (t, *J* = 8.0 Hz, 2H); ¹³C NMR (101 MHz, DMSO) δ 171.99, 149.20, 138.41, 137.98, 132.13, 129.71, 128.85, 128.81, 126.89, 116.32, 115.11, 114.10, 98.29, 45.15, 34.23; HRMS *m/z* (ESI) found [M + H]⁺ 297.1346, C₁₇H₁₇N₂O⁺ requires 297.1062; LCMS *m/z* (ESI) found [M + H]⁺ 297.1. Retention time of 2.54 min, >99% pure.

23a, 23b, 24a, and 24b were prepared with a similar procedure, as shown in Scheme 3.

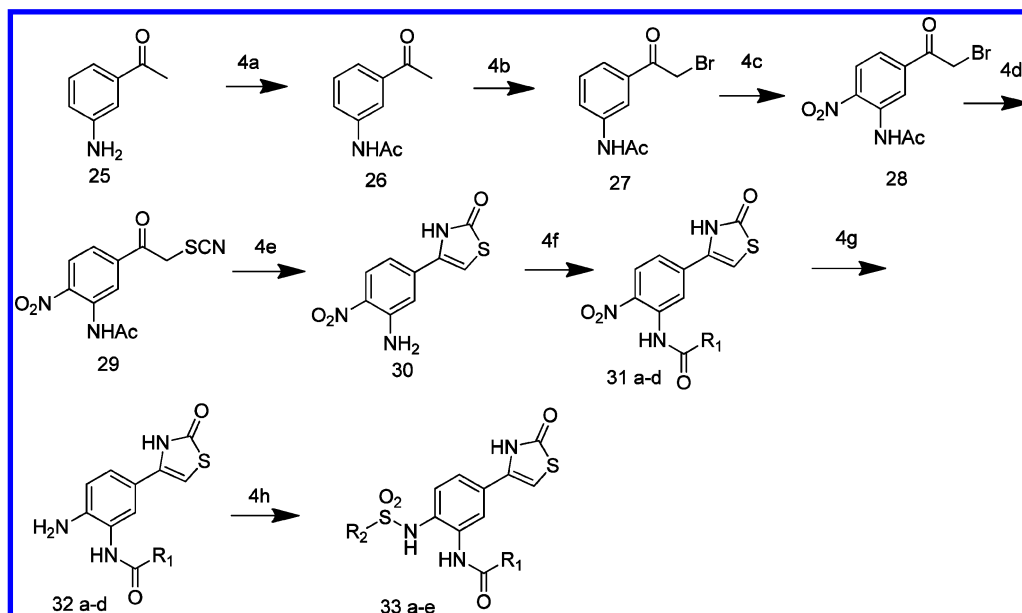
1-(4-Aminophenyl)-2-bromoethanone 23a. Mp 218–220 °C; ¹H NMR (400 MHz, DMSO) δ 11.48 (s, 1H), 7.31 (m, 2H), 6.55 (m, 2H), 6.35 (d, *J* = 1.8 Hz, 1H), 5.45 (s, 2H); ¹³C NMR (126 MHz, DMSO) δ 173.63, 149.70, 135.25, 126.41, 117.81, 114.03, 93.08; HRMS

m/z (ESI) found [M + H]⁺ 193.0458, C₉H₉N₂O⁺ requires 193.0436; LCMS *m/z* (ESI) found [M + H]⁺ 193.1. Retention time of 1.50 min, >97% pure.

4-(4-Amino-3-hydroxyphenyl)thiazol-2(3H)-one 23b. Mp 209–211 °C; ¹H NMR (400 MHz, DMSO) δ 11.44 (s, 1H), 9.20 (s, 1H), 6.85 (m, 2H), 6.56 (d, *J* = 7.8 Hz, 1H), 6.22 (s, 1H), 4.85 (s, 2H); ¹³C NMR (126 MHz, DMSO) δ 173.59, 144.23, 138.35, 135.48, 118.61, 117.61, 114.14, 111.60, 93.38; HRMS *m/z* (ESI) found [M + H]⁺ 209.0399, C₉H₉N₂O₂S⁺ requires 209.0385; LCMS *m/z* (ESI) found [M + H]⁺ 209.1.

N-(4-(2-Oxo-2,3-dihydrothiazol-4-yl)phenyl)thiophene-2-sulfonamide 24a. Mp 289–290 °C; ¹H NMR (400 MHz, DMSO) δ 11.72 (s, 1H), 10.66 (s, 1H), 7.92 (dd, *J* = 5.0, 1.4 Hz, 1H), 7.61–7.55 (m, 3H), 7.18 (m, 2H), 7.13 (dd, *J* = 5.0, 3.8 Hz, 1H), 6.69 (d, *J* = 1.9 Hz, 1H); ¹³C NMR (126 MHz, DMSO) δ 173.38, 140.21, 138.04, 134.05, 133.72, 133.09, 128.15, 126.32, 126.17, 120.47, 97.98; HRMS *m/z* (ESI) found [M + Na]⁺ 360.9757, C₁₃H₉N₂O₃NaS₂⁺ requires 360.9751; LCMS *m/z* (ESI, negative) found [M – H][–] 337.04. Retention time of 2.63 min, >94% pure.

N-(2-Hydroxy-4-(2-oxo-2,3-dihydrothiazol-4-yl)phenyl)-thiophene-2-sulfonamide 24b. Mp 219–221 °C; ¹H NMR (400 MHz, DMSO) δ 11.68 (s, 1H), 9.90 (s, 1H), 9.60 (s, 1H), 7.89 (dd, *J* = 5.0, 1.4 Hz, 1H), 7.51 (dd, *J* = 3.7, 1.4 Hz, 1H), 7.19 (d, *J* = 8.3 Hz, 1H), 7.11 (m, 1H), 7.02 (dd, *J* = 8.3, 2.1 Hz, 1H), 6.97 (d, *J* = 2.0 Hz, 1H), 6.59 (s, 1H); ¹³C NMR (126 MHz, DMSO) δ 173.35, 151.13, 141.34, 134.00, 133.52, 132.46, 128.40, 127.89, 125.37, 124.89, 116.52, 112.66, 98.29; HRMS *m/z* (ESI) found [M + H]⁺ 354.9881, C₁₃H₁₁N₂O₄S₂⁺

Scheme 4^a

^aReagents and conditions: (4a) acetic anhydride, CH_2Cl_2 , rt; (4b) CuBr_2 , EtOAc , 80°C ; (4c) nitric acid, acetic anhydride, rt; (4d) KSCN , acetone, rt; (4e) 50% H_2SO_4 , acetic acid, 100°C ; (4f) R_1COCl , pyridine, THF, rt; (4g) Fe , NH_4Cl , EtOH , 80°C ; (4h) $\text{R}_2\text{SO}_2\text{Cl}$, CH_2Cl_2 , pyridine, rt.

requires 354.9881; LCMS m/z (ESI, negative) found $[\text{M} - \text{H}]^-$ 352.9. Retention time of 2.67 min, >96% pure.

Procedure 4a of Scheme 4. 1-(3-Aminophenyl)ethanone **25** (50 g, 370 mmol) was added to a round-bottom flask. The flask was purged with argon, and dry CH_2Cl_2 (300 mL) was added. Acetic anhydride (41.9 mL, 444 mmol) was added. The mixture was stirred at room temperature and the reaction monitored by TLC. Upon completion, the reaction mixture was washed with a saturated solution of sodium carbonate, and the organic layers were dried over Na_2SO_4 and concentrated under reduced pressure. The product *N*-(3-(2-bromoacetyl)phenyl)acetamide **26** was obtained in quantitative yield (65.6 g). ^1H NMR (400 MHz, CDCl_3) δ 8.28 (s, 1H), 8.04 (s, 1H), 7.98 (d, $J = 8.3$ Hz, 1H), 7.67 (d, $J = 7.7$ Hz, 1H), 7.42 (t, $J = 7.9$ Hz, 1H), 2.60 (s, 3H), 2.23 (s, 3H); LCMS m/z (ESI) found $[\text{M} + \text{H}]^+$ 178.1. Retention time of 2.10 min, >98% pure.

Procedure 4b of Scheme 4. Following the same procedure 2a in Scheme 2, **26** (25 g, 141 mmol) gave *N*-(3-(2-bromoacetyl)phenyl)acetamide **27** (22 g, 86 mmol, 60.9% yield). ^1H NMR (400 MHz, CDCl_3) δ 8.08 (d, $J = 1.8$ Hz, 1H), 7.93 (dd, $J = 8.1, 1.2$ Hz, 1H), 7.70 (d, $J = 7.8$ Hz, 1H), 7.44 (t, $J = 8.0$ Hz, 1H), 4.47 (s, 2H), 2.23 (s, 3H); LCMS m/z (ESI) found $[\text{M} + \text{H}]^+$ 256.03. Retention time of 2.36 min, >99% pure.

Procedure 4c of Scheme 4. Nitric acid (0.209 mL, 4.69 mmol) was added dropwise to acetic anhydride (4 mL, 42.4 mmol) at 0°C and stirred for 15 min. **27** (0.8 g, 3.12 mmol) was then added portionwise and the reaction mixture allowed to warm to room temperature. After being stirred at room temperature for 2 h, the reaction mixture was poured into ice (10 mL). CH_2Cl_2 (50 mL) was added and the organic layer was separated, dried over Na_2SO_4 , filtered, and evaporated to give the crude residue. This was purified by column chromatography (gradient elution, gradient 5–30% EtOAc /petroleum ether) to give *N*-(3-(2-bromoacetyl)-4-nitrophenyl)acetamide **28** (0.376 g, 1.250 mmol, 40% yield). ^1H NMR (400 MHz, CDCl_3) δ 10.27 (s, 1H), 9.41 (d, $J = 1.9$ Hz, 1H), 8.30 (d, $J = 8.8$ Hz, 1H), 7.76 (dd, $J = 8.8, 1.9$ Hz, 1H), 4.50 (s, 2H), 2.34 (s, 3H); LCMS m/z (ESI, negative) found $[\text{M} - \text{H}]^-$ 300.8.

Procedures 4d and 4e of Scheme 4. Following the same procedures 2b and 2c in Scheme 2, **28** (0.5 g, 1.661 mmol) afforded 4-(3-amino-4-nitrophenyl)thiazol-2(3H)-one **30** (0.21 g, 0.885 mmol, 53.3% yield) as a powdery yellow solid. ^1H NMR (400 MHz, DMSO) δ 11.94 (s, 1H), 8.00 (d, $J = 9.0$ Hz, 1H), 7.47 (s, 2H), 7.17 (d, $J = 1.9$ Hz, 1H), 6.93 (s,

1H), 6.88 (dd, $J = 9.0, 1.9$ Hz, 1H); LCMS m/z (ESI) found $[\text{M}]^+$ 237.2. Retention time of 2.57 min, >94% pure.

Procedure 4f of Scheme 4. To a solution of **30** (0.5 g, 2.108 mmol) in THF (20 mL) and pyridine (1 mL, 12.36 mmol) was added 2-phenylacetyl chloride (0.558 mL, 4.22 mmol) at room temperature under a nitrogen atmosphere. The resulting mixture was allowed to stir for 2 h. Upon completion of the reaction, the crude mixture was diluted with EtOAc and washed with water followed by 1 N HCl (20 mL). The resulting organic layer was then dried over Na_2SO_4 and concentrated under reduced pressure. Purification by silica gel column chromatography (gradient elution, gradient 0–5% $\text{MeOH}/\text{CH}_2\text{Cl}_2$) gave *N*-(2-nitro-5-(2-oxo-2,3-dihydrothiazol-4-yl)phenyl)-2-phenylacetamide **31a** (0.45 g, 1.266 mmol, 60.1% yield). ^1H NMR (400 MHz, DMSO) δ 12.03 (s, 1H), 10.51 (s, 1H), 8.03 (d, $J = 8.7$ Hz, 1H), 7.98 (d, $J = 1.9$ Hz, 1H), 7.61 (dd, $J = 8.6, 1.9$ Hz, 1H), 7.37–7.26 (m, 5H), 7.08 (s, 1H), 3.73 (s, 2H).

Compounds **31b–d** were prepared according to the general procedure 4f.

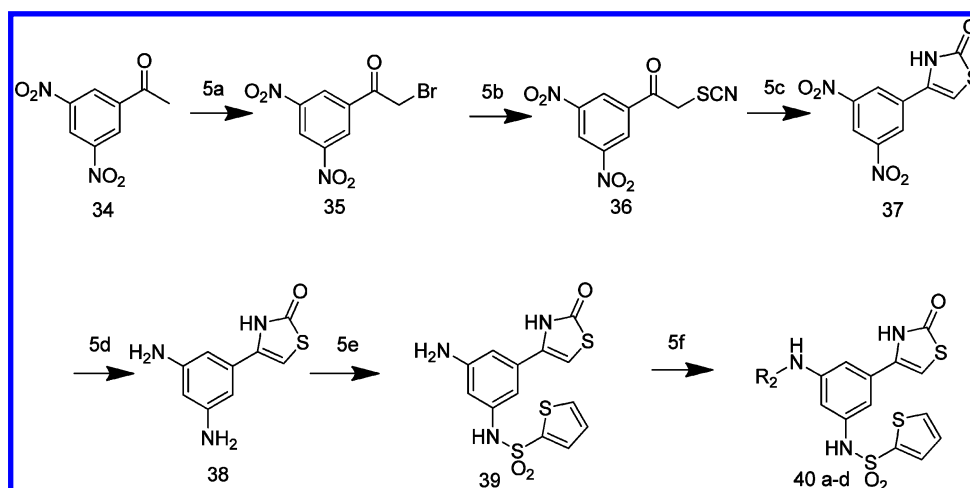
N-(2-Nitro-5-(2-oxo-2,3-dihydrothiazol-4-yl)phenyl)-3-phenylpropanamide 31b. ^1H NMR (400 MHz, DMSO) δ 12.03 (s, 1H), 10.36 (s, 1H), 8.03 (d, $J = 8.6$ Hz, 1H), 7.89 (d, $J = 1.9$ Hz, 1H), 7.61 (dd, $J = 8.7, 2.0$ Hz, 1H), 7.35–7.23 (m, 4H), 7.21 (d, $J = 6.9$ Hz, 1H), 7.06 (s, 1H), 2.91 (t, $J = 7.7$ Hz, 2H), 2.68 (t, $J = 7.8$ Hz, 2H); LCMS m/z (ESI, negative) found $[\text{M} - \text{H}]^-$ 368.1. Retention time of 3.31 min, >98% pure.

N-(2-Nitro-5-(2-oxo-2,3-dihydrothiazol-4-yl)phenyl)-butyramide 31c. ^1H NMR (400 MHz, DMSO) δ 12.02 (s, 1H), 10.29 (s, 1H), 8.01 (d, $J = 8.7$ Hz, 1H), 7.88 (d, $J = 1.9$ Hz, 1H), 7.61 (dd, $J = 8.6, 2.0$ Hz, 1H), 7.07 (d, $J = 1.7$ Hz, 1H), 2.33 (t, $J = 7.3$ Hz, 2H), 1.61 (m, 2H), 0.94 (t, $J = 7.4$ Hz, 3H); LCMS m/z (ESI, negative) found $[\text{M} - \text{H}]^-$ 306.1. Retention time of 2.93 min, >95% pure.

N-(2-Nitro-5-(2-oxo-2,3-dihydrothiazol-4-yl)phenyl)-cyclopentanecarboxamide 31d. ^1H NMR (400 MHz, DMSO) δ 12.02 (s, 1H), 10.29 (s, 1H), 8.01 (d, $J = 8.7$ Hz, 1H), 7.88 (d, $J = 2.0$ Hz, 1H), 7.60 (dd, $J = 8.7$ Hz, 1.9 Hz, 1H), 7.08 (s, 1H), 2.85 (m, 1H), 1.85 (m, 2H), 1.74 (m, 2H), 1.65 (m, 2H), 1.57 (m, 2H); LCMS m/z (ESI, negative) found $[\text{M} - \text{H}]^-$ 332.08. Retention time of 3.24 min, >96% pure.

Procedure 4g of Scheme 4. Compounds **32a–d** were prepared according to the general procedure 2d in Scheme 2.

N-(2-Amino-5-(2-oxo-2,3-dihydrothiazol-4-yl)phenyl)-2-phenylacetamide 32a. ^1H NMR (400 MHz, DMSO) δ 11.51 (s, 1H), 9.41 (s, 1H), 7.46 (s, 1H), 7.39–7.31 (m, 4H), 7.25 (m, 1H), 7.22 (m, 1H), 6.72

Scheme 5^a

^aReagents and conditions: (5a) CuBr₂, EtOAc, 80 °C; (5b) KSCN, acetone, rt; (5c) 50% H₂SO₄, acetic acid, 100 °C; (5d) Fe, NH₄Cl, EtOH, 80 °C; (5e) thiophene-2-sulfonyl chloride, CH₂Cl₂, pyridine, rt; (5f) R₂COCl, pyridine, CH₂Cl₂, rt.

(d, *J* = 8.2 Hz, 1H), 6.35 (s, 1H), 5.19 (s, 2H), 3.67 (s, 2H); LCMS *m/z* (ESI) found [M + H]⁺ 326.1.

N-(2-Amino-5-(2-oxo-2,3-dihydrothiazol-4-yl)phenyl)-3-phenylpropanamide 32b. ¹H NMR (400 MHz, DMSO) δ 11.51 (s, 1H), 9.17 (s, 1H), 7.44 (d, *J* = 1.9 Hz, 1H), 7.33–7.25 (m, 4H), 7.20 (dd, *J* = 8.3, 2.1 Hz, 2H), 6.70 (d, *J* = 8.4 Hz, 1H), 6.34 (s, 1H), 5.10 (s, 2H), 2.92 (t, *J* = 7.8 Hz, 2H), 2.64 (t, *J* = 7.8 Hz, 2H); LCMS *m/z* (ESI) found [M + H]⁺ 340.06.

N-(2-Amino-5-(2-oxo-2,3-dihydrothiazol-4-yl)phenyl)-butyramide 32c. ¹H NMR (400 MHz, DMSO) δ 11.51 (s, 1H), 9.13 (s, 1H), 7.46 (d, *J* = 1.9 Hz, 1H), 7.20 (dd, *J* = 8.4, 2.1 Hz, 1H), 6.72 (d, *J* = 8.4 Hz, 1H), 6.35 (d, *J* = 1.6 Hz, 1H), 5.15 (s, 2H), 2.30 (t, *J* = 7.3 Hz, 2H), 1.62 (m, 2H), 0.94 (t, *J* = 7.4 Hz, 3H); LCMS *m/z* (ESI) found [M + H]⁺ 278.0. Retention time of 2.09 min, >96% pure.

N-(2-Amino-5-(2-oxo-2,3-dihydrothiazol-4-yl)phenyl)-cyclopentanecarboxamide 32d. ¹H NMR (400 MHz, DMSO) δ 11.51 (s, 1H), 9.13 (s, 1H), 7.48 (d, *J* = 2.2 Hz, 1H), 7.19 (dd, *J* = 8.4, 2.1 Hz, 1H), 6.72 (d, *J* = 8.4 Hz, 1H), 6.36 (d, *J* = 1.8 Hz, 1H), 5.13 (s, 2H), 2.83 (m, 1H), 1.86 (m, 2H), 1.77–1.64 (m, 4H), 1.55 (m, 2H); LCMS *m/z* (ESI) found [M + H]⁺ 304.0. Retention time of 2.32 min, >95% pure.

Procedure 4h of Scheme 4. Compounds 33a–e were prepared according to the general procedure 2e in Scheme 2.

N-(5-(2-Oxo-2,3-dihydrothiazol-4-yl)-2-(thiophene-2-sulfonamido)phenyl)-2-phenylacetamide 33a. Mp 182–184 °C; ¹H NMR (400 MHz, DMSO) δ 11.77 (s, 1H), 9.78 (s, 1H), 9.52 (s, 1H), 7.92 (d, *J* = 4.9 Hz, 1H), 7.88 (s, 1H), 7.36 (m, 6H), 7.28 (m, 1H), 7.21 (d, *J* = 8.5 Hz, 1H), 7.10 (t, *J* = 4.2 Hz, 1H), 6.70 (s, 1H), 3.61 (s, 2H); ¹³C NMR (126 MHz, DMSO) δ 173.25, 169.77, 140.24, 135.79, 134.15, 133.46, 133.36, 132.89, 129.79, 128.77, 128.43, 128.23, 127.09, 126.94, 122.01, 120.95, 99.28, 43.18; HRMS *m/z* (ESI) found [M + H]⁺ 472.0463, C₂₁H₁₈N₃O₄S₃⁺ requires 472.0459; LCMS *m/z* (ESI) found [M + H]⁺ 472.0. Retention time of 3.13 min, >99% pure.

N-(5-(2-Oxo-2,3-dihydrothiazol-4-yl)-2-(thiophene-2-sulfonamido)phenyl)-3-phenylpropanamide 33b. Mp 101–103 °C; ¹H NMR (400 MHz, DMSO) δ 11.78 (s, 1H), 9.70 (s, 1H), 9.35 (s, 1H), 7.92 (d, *J* = 4.7 Hz, 1H), 7.86 (s, 1H), 7.40 (m, 2H), 7.27 (m, 6H), 7.10 (t, *J* = 4.2 Hz, 1H), 6.70 (s, 1H), 2.86 (t, *J* = 7.9 Hz, 2H), 2.55 (t, *J* = 7.9 Hz, 2H); ¹³C NMR (126 MHz, DMSO) δ 173.58, 171.56, 141.21, 140.07, 134.14, 133.41, 133.19, 132.94, 128.86, 128.67, 128.39, 128.30, 126.93, 126.52, 122.16, 120.95, 99.41, 37.89, 31.01; HRMS *m/z* (ESI) found [M + H]⁺ 486.0619, C₂₂H₂₀N₃O₄S₃⁺ requires 486.0616; LCMS *m/z* (ESI) found [M + H]⁺ 486.0. Retention time of 3.27 min, >98% pure.

N-(5-(2-Oxo-2,3-dihydrothiazol-4-yl)-2-(thiophene-2-sulfonamido)phenyl)butyramide 33c. Mp 142–143 °C; ¹H NMR (400 MHz, DMSO) δ 11.79 (s, 1H), 9.68 (s, 1H), 9.27 (s, 1H), 7.93 (d, *J*

= 4.9 Hz, 1H), 7.87 (s, 1H), 7.44 (d, *J* = 2.5 Hz, 1H), 7.39 (d, *J* = 8.8 Hz, 1H), 7.23 (d, *J* = 8.4 Hz, 1H), 7.12 (m, 1H), 6.72 (s, 1H), 2.22 (t, *J* = 7.2 Hz, 2H), 1.57 (m, 2H), 0.92 (t, *J* = 7.3 Hz, 3H); ¹³C NMR (126 MHz, DMSO) δ 173.69, 172.51, 139.96, 134.22, 133.41, 132.98, 128.58, 128.35, 128.18, 127.23, 122.17, 121.03, 99.57, 38.26, 18.83, 13.99; HRMS *m/z* (ESI) found [M + H]⁺ 424.0461, C₁₇H₁₈N₃O₄S₃⁺ requires 424.0459; LCMS *m/z* (ESI) found [M + H]⁺ 424.0. Retention time of 2.93 min, >99% pure.

N-(5-(2-Oxo-2,3-dihydrothiazol-4-yl)-2-(thiophene-2-sulfonamido)phenyl)cyclopentanecarboxamide 33d. Mp 207–209 °C; ¹H NMR (400 MHz, DMSO) δ 11.60 (s, 1H), 9.20 (s, 1H), 8.15 (s, 1H), 7.70 (s, 1H), 7.31 (d, *J* = 2.7 Hz, 1H), 7.16 (m, 2H), 7.01 (t, *J* = 4.2 Hz, 1H), 6.44 (s, 1H), 2.73 (m, 1H), 1.85 (m, 2H), 1.70 (m, 4H), 1.58 (m, 2H); HRMS *m/z* (ESI) found [M + H]⁺ 450.0325, C₁₉H₂₀N₃O₄S₃⁺ requires 450.0616; LCMS *m/z* (ESI) found [M + H]⁺ 449.91. Retention time of 3.15 min, >96% pure.

N-(5-(2-Oxo-2,3-dihydrothiazol-4-yl)-2-(phenylmethylsulfonamido)phenyl)cyclopentanecarboxamide 33e. Mp 245–247 °C; ¹H NMR (400 MHz, DMSO) δ 11.81 (s, 1H), 9.39 (s, 1H), 9.00 (s, 1H), 7.90 (d, *J* = 1.5 Hz, 1H), 7.45–7.38 (m, 2H), 7.37–7.30 (m, 5H), 6.74 (d, *J* = 1.6 Hz, 1H), 4.49 (s, 2H), 2.78 (m, 1H), 1.85 (m, 2H), 1.70 (m, 7.3 Hz, 4H), 1.60–1.50 (m, 2H); ¹³C NMR (126 MHz, DMSO) δ 175.55, 173.37, 133.60, 132.10, 131.38, 129.99, 129.69, 128.86, 128.76, 127.40, 124.79, 122.37, 121.79, 98.76, 58.30, 45.41, 30.43, 26.11; HRMS *m/z* (ESI) found [M + H]⁺ 458.1218, C₂₂H₂₄N₃O₄S₂⁺ requires 458.1208; LCMS *m/z* (ESI) found [M + H]⁺ 458.0. Retention time of 3.23 min, >99% pure.

Compound 38. Following the same procedures 2a, 2b, 2c, and 2d in Scheme 2 gave 4-(3,5-diaminophenyl)thiazol-2(3H)-one 38. Mp 193–194 °C; ¹H NMR (400 MHz, DMSO) δ 11.43 (s, 1H), 6.30 (d, *J* = 1.4 Hz, 1H), 5.98 (d, *J* = 1.9 Hz, 2H), 5.84 (t, *J* = 1.9 Hz, 1H), 4.85 (s, 4H); ¹³C NMR (126 MHz, DMSO) δ 173.38, 149.85, 136.28, 131.43, 100.70, 96.33; HRMS *m/z* (ESI) found [M + H]⁺ 208.0601, C₉H₁₀N₃O₂S⁺ requires 208.0545; LCMS *m/z* (ESI) found [M + H]⁺ 208.12. Retention time of 0.90 min, >97% pure.

Compound 39. Following the same procedure 2e in Scheme 2, 38 (1g, 4.83 mmol) gave N-(3-amino-5-(2-oxo-2,3-dihydrothiazol-4-yl)-phenyl)thiophene-2-sulfonamide 39 (0.563 g, 1.592 mmol, 33% yield). Mp 253–254 °C; ¹H NMR (400 MHz, DMSO) δ 11.62 (s, 1H), 10.24 (s, 1H), 7.89 (dd, *J* = 5.0, 1.4 Hz, 1H), 7.58 (dd, *J* = 3.7, 1.4 Hz, 1H), 7.12 (dd, *J* = 5.0, 3.7 Hz, 1H), 6.52 (t, *J* = 1.7 Hz, 1H), 6.43 (t, *J* = 1.7 Hz, 1H), 6.41 (d, *J* = 1.9 Hz, 1H), 6.36 (d, *J* = 1.1 Hz, 1H), 5.33 (s, 2H); ¹³C NMR (101 MHz, DMSO) δ 173.31, 150.05, 140.47, 138.98, 135.06, 133.57, 132.75, 131.62, 127.94, 107.55, 106.00, 105.33, 97.96; HRMS *m/z* (ESI) found [M + H]⁺ 354.0059, C₁₃H₁₂N₃O₃S₃⁺ requires 354.0041; LCMS

m/z (ESI) found $[M + H]^+$ 354.0. Retention time of 2.26 min, >99% pure.

Procedure 5f of Scheme 5. To a solution of **39** (95 mg, 0.269 mmol) in CH_2Cl_2 (10 mL) and pyridine (0.109 mL, 1.344 mmol) was added thiophene-2-carbonyl chloride (47.3 mg, 0.323 mmol) at room temperature under a nitrogen atmosphere. The resulting mixture was allowed to stir for 2 h. Upon completion of the reaction, the crude mixture was diluted with CH_2Cl_2 and washed with water followed by 1 N HCl (10 mL). The resulting organic layer was then dried over Na_2SO_4 and concentrated under reduced pressure. Purification by silica gel column chromatography (gradient elution, gradient 0–5% MeOH/ CH_2Cl_2) gave *N*-(3-(2-oxo-2,3-dihydrothiazol-4-yl)-5-(thiophene-2-sulfonamido)phenyl)thiophene-2-carboxamide **40a**. Mp 266–267 °C; ^1H NMR (400 MHz, DMSO) δ 11.84 (s, 1H), 10.81–10.48 (br s, 1H), 10.40 (s, 1H), 8.04 (d, J = 3.3 Hz, 1H), 7.94–7.84 (m, 2H), 7.73 (s, 1H), 7.66 (d, J = 2.9 Hz, 1H), 7.62 (s, 1H), 7.24 (m, 1H), 7.21–7.07 (m, 2H), 6.55 (s, 1H); ^{13}C NMR (126 MHz, DMSO) δ 173.35, 160.45, 140.25, 140.20, 140.07, 138.82, 134.24, 133.98, 133.13, 132.72, 131.51, 129.94, 128.59, 128.12, 114.18, 113.10, 112.71, 99.46; HRMS m/z (ESI) found $[M + H]^+$ 463.9862, $\text{C}_{18}\text{H}_{14}\text{N}_3\text{O}_4\text{S}_4^+$ requires 463.9867; LCMS m/z (ESI, negative) found $[M - H]$ 462.1. Retention time of 3.26 min, >98% pure.

Compounds **40b–d** were prepared according to the general procedure 5f.

3-Cyclohexyl-N-(3-(2-oxo-2,3-dihydrothiazol-4-yl)-5-(thiophene-2-sulfonamido)phenyl)propanamide 40b. Mp 122–124 °C; ^1H NMR (400 MHz, DMSO) δ 11.80 (s, 1H), 10.57 (s, 1H), 10.01 (s, 1H), 7.91 (d, J = 4.9 Hz, 1H), 7.62 (d, J = 3.7 Hz, 1H), 7.58 (s, 1H), 7.43 (s, 1H), 7.12 (m, 1H), 7.01 (s, 1H), 6.48 (s, 1H), 2.30 (t, J = 15.1, 7.2 Hz, 2H), 1.71–1.65 (m, 5H), 1.47 (dd, J = 15.1, 7.2 Hz, 2H), 1.23–1.15 (m, 4H), 0.94–0.80 (m, 2H); ^{13}C NMR (126 MHz, DMSO) δ 173.37, 172.23, 140.82, 140.21, 138.77, 134.40, 133.95, 133.10, 131.60, 128.08, 112.75, 112.38, 111.35, 99.28, 37.19, 34.37, 33.04, 32.94, 26.56, 26.21; HRMS m/z (ESI) found $[M + H]^+$ 492.1093, $\text{C}_{22}\text{H}_{26}\text{N}_3\text{O}_4\text{S}_3^+$ requires 492.1085; LCMS m/z (ESI, negative) found $[M - H]$ 492.1. Retention time of 3.91 min, >97% pure.

N-(3-(2-Oxo-2,3-dihydrothiazol-4-yl)-5-(thiophene-2-sulfonamido)phenyl)-3-phenylpropanamide 40c. Mp 120–122 °C; ^1H NMR (400 MHz, DMSO) δ 11.81 (s, 1H), 10.59 (s, 1H), 10.08 (s, 1H), 7.91 (dd, J = 5.0, 1.2 Hz, 1H), 7.62 (dd, J = 3.7, 1.3 Hz, 1H), 7.58 (s, 1H), 7.43 (s, 1H), 7.30–7.23 (m, 4H), 7.18 (t, J = 7.0 Hz, 1H), 7.13 (dd, J = 4.9, 3.8 Hz, 1H), 7.02 (t, J = 1.7 Hz, 1H), 6.48 (s, 1H), 2.89 (t, J = 7.7 Hz, 2H), 2.62 (t, J = 7.7 Hz, 2H); ^{13}C NMR (126 MHz, DMSO) δ 173.38, 171.13, 141.53, 140.68, 140.18, 138.80, 134.35, 133.97, 133.12, 131.64, 128.79, 128.69, 128.10, 126.43, 112.70, 112.47, 111.34, 99.36, 38.32, 31.13; HRMS m/z (ESI) found $[M + H]^+$ 486.0620, $\text{C}_{22}\text{H}_{20}\text{N}_3\text{O}_4\text{S}_3^+$ requires 486.0616; LCMS m/z (ESI) found $[M + H]^+$ 486.0. Retention time of 3.17 min, >98% pure.

N-(3-(2-Oxo-2,3-dihydrothiazol-4-yl)-5-(thiophene-2-sulfonamido)phenyl)butyramide 40d. Mp 91–93 °C; ^1H NMR (400 MHz, DMSO) δ 11.80 (s, 1H), 10.58 (s, 1H), 10.02 (s, 1H), 7.91 (dd, J = 5.0, 1.3 Hz, 1H), 7.63 (dd, J = 3.7, 1.4 Hz, 1H), 7.59 (s, 1H), 7.43 (s, 1H), 7.13 (dd, J = 5.0, 3.8 Hz, 1H), 7.01 (t, J = 1.7 Hz, 1H), 6.48 (s, 1H), 2.27 (t, J = 7.3 Hz, 2H), 1.59 (m, 2H), 0.90 (t, J = 7.4 Hz, 3H); ^{13}C NMR (101 MHz, DMSO) δ 173.34, 171.84, 140.70, 140.16, 138.79, 134.33, 133.88, 133.04, 131.52, 128.04, 112.66, 112.32, 111.31, 99.25, 18.86, 14.01; HRMS m/z (ESI) found $[M + H]^+$ 424.0462, $\text{C}_{17}\text{H}_{18}\text{N}_3\text{O}_4\text{S}_3^+$ requires 424.0459; LCMS m/z (ESI) found $[M + H]^+$ 424.0. Retention time of 2.83 min, >98% pure.

Computer Docking for Fragment Enrichment. Docking studies were performed using the Schrödinger suite.³¹ The protein structure of BRD4 in complex with JQ1 was used to build the docking grid (PDB code 3MXF). The X-ray structure was preprocessed using the protein preparation module, and a 20 Å grid was built around the active site as defined by the position of JQ1. Water molecules around the binding site were retained because of the very important water hydrogen bonding network located at the bottle of the binding site. The compounds in our fragment library were prepared using the Ligprep module to obtain energy minimized 3D structures, which were then screened in Glide,³² using the standard precision scoring algorithm. Then the binding

conformations were manually checked by experts. Through a scrutiny for the existence of the essential hydrogen bonding with Asn140 in BRD4, a total of 41 compounds were selected for further crystallization.

Protein Expression. The BRD4(1) protein expression was generally followed by the protocol of Filippakopoulos et al.⁷ Colonies from freshly transformed plasmid DNA in *E. coli* BL21(DE3) condon plus RIL cells were grown overnight at 37 °C in 50 mL of Terrific Broth medium with 50 $\mu\text{g}/\text{mL}$ kanamycin and 34 $\mu\text{g}/\text{mL}$ chloramphenicol (startup culture). Then the startup culture was diluted 100-fold in 1 L of fresh TB medium and cell growth was at 37 °C to an optical density of about 0.8 at OD₆₀₀ before the temperature was decreased to 16 °C. When the system equilibrated at 16 °C, the optical density was about 1.2 at OD₆₀₀ and protein expression was induced overnight at 16 °C with 0.2 mM isopropyl- β -D-thiogalactopyranoside (IPTG). The bacteria were harvested by centrifugation (4000g for 20 min at 4 °C) and were frozen at –80 °C as pellets for storage. Cells expressing His6-tagged proteins were resuspended in lysis buffer (50 mM HEPES, pH 7.5 at 25 °C, 500 mM NaCl, 10 mM imidazole, 5% glycerol with freshly added 0.5 mM TCEP (tris(2-carboxyethyl)phosphine hydrochloride), and 1 mM PMSF (phenylmethanesulfonyl fluoride)) and lysed using an JN 3000 PLUS high pressure homogenizer (JNBIO, Guangzhou, China) at 4 °C. The lysate was cleared by centrifugation (12000g for 1 h at 4 °C) and was applied to a nickel nitrilotriacetic acid agarose column. The column was washed once with 50 mL of wash buffer containing 30 mM imidazole. The protein was eluted using a step elution of imidazole in elution buffer (100 and 250 mM imidazole in 50 mM HEPES, pH 7.5 at 25 °C, 500 mM NaCl, 5% glycerol). All fractions were collected and monitored by SDS–polyacrylamide gel electrophoresis (Bio-Rad Criterion Precast Gels, 4–12% Bis-Tris, 1.0 mm, from Bio-Rad, CA). After the addition of 1 mM dithiothreitol (DTT), the eluted protein was treated overnight at 4 °C with tobacco etch virus (TEV) protease to remove the His6 tag. The protein was concentrated and further purified with size exclusion chromatography on a Superdex 75 16/60 HiLoad gel filtration column. Samples were monitored by SDS–polyacrylamide gel electrophoresis and concentrated to 8–10 mg/mL in the gel filtration buffer, 10 mM Hepes, pH 7.5, 500 mM NaCl, 1 mM DTT, and were used for enzymatic assay and crystallization.

Crystallization and Data Collection. Aliquots of the purified proteins were set up for crystallization using the vapor diffusion method. BRD4(1) crystals were grown by mixing 1 μL of the protein (9 mg/mL) with an equal volume of reservoir solution containing 6 M sodium formate and 10% glycerol. Its complex with 41 fragments was grown at 4 °C in 1 μL of protein (10 mg/mL + 5 mM fragment) with an equal volume of reservoir solution containing 6 M sodium formate and 10% glycerol. Crystals grew to diffracting quality within 1–3 weeks in all cases.

Data were collected at 100 K on beamline BL17U (at wavelength 0.9793 Å) at the Shanghai Synchrotron Radiation Facility (SSRF) (Shanghai, China) for the cocrystallized structures. The data were processed with the HKL2000,³³ software packages, and the structures were then solved by molecular replacement, using the CCP4 program MOLREP. The search model used for the crystals was the BRD4-JQ1 complex structure (PDB code 3MXF). The structures were refined using the CCP4 program REFMAC³⁴ combined with the simulated-annealing protocol implemented in the program PHENIX.³⁵ With the aid of the program Coot,³⁶ compound, water molecules, and others were fitted into the initial $F_o - F_c$ maps. The complete statistics, as well as the quality of the solved structures, are shown in Table S2.

Fluorescence Anisotropy Binding Assay. The binding of compounds to BRD4 was assessed using a fluorescence anisotropy binding assay. The fluorescent ligand was prepared by attaching a fluorescent fragment (fluorescein isothiocyanate isomer I, 5-FIFC, CAS number 3326-32-7) to the (+)-JQ1 (the details of synthesis and spectra of the ligand are provided in Supporting Information Scheme S1). Generally the method involves incubating the bromodomain protein BRD4, fluorescent ligand, and a variable concentration of test compound together to reach thermodynamic equilibrium under conditions such that in the absence of test compound the fluorescent ligand is significantly (>50%) bound and in the presence of a sufficient

concentration of a potent inhibitor the anisotropy of the unbound fluorescent ligand is measurably different from the bound value.

All components were dissolved in buffer of composition 50 mM HEPES, pH 7.4, 150 mM NaCl, and 0.5 mM CHAPS with final concentrations of 45 nM BRD4(1) and 5 nM fluorescent ligand. This reaction mixture was added to various concentrations of test compound or DMSO vehicle (5% final) in a Corning 384-well black low volume plate (CLS3575) and equilibrated in the dark for 4 h at room temperature. Fluorescence anisotropy was read on a BioTek Synergy2 multimode microplate reader ($\lambda_{\text{ex}} = 485 \text{ nm}$, $\lambda_{\text{em}} = 530 \text{ nm}$; dichroic, 505 nm).

In Vitro PK Study. Microsomes (human microsomes, Xenotech, lot no. H0610; rat microsomes, Xenotech, lot no. R1000) (0.5 mg/mL) were preincubated with 1 μM test compound for 5 min at 37 °C in 0.1 M phosphate buffer (pH 7.4) with 1 mM EDTA and 5 mM MgCl_2 . The reactions were initiated by adding prewarmed cofactors (1 mM NADPH). After 0, 5, 10, and 30 min incubations at 37 °C, the reactions were stopped by adding an equal volume of cold acetonitrile. The samples were vortexed for 10 min and then centrifuged at 10000g for 10 min. Supernatants were analyzed by LC/MS/MS for the amount of parent compound remaining, and the corresponding loss of parent compound was also determined by LC/MS/MS.

The CYP enzymatic activities were characterized based on their probe reactions: CYP3A4 (midazolam), CYP2D6 (dextromethorphan), CYP2C9 (diclofenac), CYP1A2 (phenacetin), and CYP2C19 (mephenytoin). Incubation mixtures were prepared in a total volume of 100 μL with the following: 0.2 mg/mL microsome (human microsome, Xenotech, lot no. H0610), NADPH (1 mM), 100 mM phosphate buffer (pH 7.4), probe substrates cocktail (midazolam 10 μM , testosterone 100 μM , dextromethorphan 10 μM , diclofenac 20 μM , phenacetin 100 μM , mephenytoin 100 μM), and 10 μM tested compound or positive control cocktail (ketoconazole 10 μM , quinidine 10 μM , sulfaphenazole 100 μM , naphthoflavone 10 μM , tranylcypromine 1000 μM) or negative control (PBS). The final concentration of organic reagent in incubation mixtures was less than 1% v/v. There was a 5 min preincubation period at 37 °C before the reaction was initiated by adding a NADPH-generating system. Reactions were conducted for 20 min for CYPs. For each probe drug, the percentage of metabolite conversion was less than 20% of substrate added. The inhibition rate was calculated as [(the formation of the metabolite of probe substrates with 10 μM tested compound)/(the formation of the metabolite of probe substrates with PBS)] \times 100.

Cellular Assays. Cell Culture and Compounds. Human colon cancer HT-29 cells were purchased from the American Type Culture Collection. The cells were cultured in McCoy's 5A medium (modified) supplemented with 10% FBS (Life Technologies) at 37 °C in a humidified atmosphere containing 5% CO_2 . Compounds were dissolved in DMSO at 0.01 mol/L as stock solution, which was diluted to desired concentrations with normal saline.

Growth Inhibition Assays. The growth inhibition of compounds was examined by sulforhodamine B (SRB) assays.³⁷ Briefly, cells seeded in 96-well plates were treated in triplicate with gradient concentrations of tested compounds at 37 °C for 72 h and then assessed with SRB (Sigma). The absorbance at 560 nm was detected with a plate reader (SpectraMax, Molecular Devices). The inhibition rate was calculated as [(A₅₆₀ treated/A₅₆₀ control)] \times 100.

Quantitative Real Time PCR (RT-qPCR) Analyses. HT-29 cells were seeded into six-well plates and incubated overnight. Cells were treated with compounds at a final concentration of 10 μM for 24 h. Total RNA was isolated with the Trizol reagent (Invitrogen) and reverse-transcribed using PrimeScript RTase (Takara). cDNA was used for RT-qPCR SYBR Green assays (Takara) with the following primers (synthesized by Sangon Corporation): β -actin primer, 5'-GGATGCA-GAAGGAGATCACTG-3' (forward), 5'-CGATCCACACGGAGTA-CTTG-3' (backward); c-myc primer, 5'-CGTCTCCACATCAG-CACAA-3' (forward), 5'-TGTTGGCAGCAGGATAGTCCTT-3' (backward). The relative levels of c-myc mRNA were calculated as [(c-myc mRNA in the treatment group)/(β -actin mRNA in the treatment group)]/[(c-myc mRNA in the control group)/(β -actin mRNA in the control group)].

■ ASSOCIATED CONTENT

Supporting Information

Competitive binding assay results of fragment hits and statistics of eight crystal structures. This material is available free of charge via the Internet at <http://pubs.acs.org>.

■ AUTHOR INFORMATION

Corresponding Author

*For B.X.: phone, +86 21 50806600, extension 5412; fax, +86 21 50807088; e-mail, bxiong@mail.shcnc.ac.cn. For J.H.: e-mail, hejh@sinap.ac.cn. For J.S.: e-mail, jkshen@mail.shcnc.ac.cn.

Author Contributions

[†]L.Z., D.C., T.C., and Y.W. contributed equally.

Notes

The authors declare no competing financial interest.

■ ACKNOWLEDGMENTS

The authors thank Prof. Albert Berghuis and Mingyue Zheng for their helps in preparing the manuscript and thank Dr. Haiyan Liu for performing the in vitro PK study. We are grateful for financial support from Program of Excellent Young Scientist of Chinese Academy of Sciences to B.X. (Grant KSCX2-EW-Q-3-01), "Interdisciplinary Cooperation Team" Program for Science and Technology Innovation of the Chinese Academy of Sciences, the "100 Talents Project" of CAS to Y.X., The National Natural Science Foundation of China (Grants 81072580, 91013010, and 21172233), and National Program on Key Basic Research Project (973 Program, Grant 2009CB940903).

■ ABBREVIATIONS USED

FBDD, fragment based drug discovery; PTM, post-translational modification; HAT, histone acetyltransferase; HDAC, histone deacetylase; KAc, acetylated lysine; BET, bromodomain and extra-terminal; P-TEFb, positive transcription elongation factor complex; NUT, nuclear protein in testis; CNS, central nervous system; BRD4(I), first bromodomain of BRD4; GSK, GlaxoSmithKline; DSF, differential scanning fluorimetry; STD, saturation transfer difference; WaterLOGSY, water–ligand observed via gradient spectroscopy; CPMG, Carr–Purcell–Meiboom–Gill; SPR, surface plasmon resonance; PSA, polar surface area; SSRF, Shanghai Synchrotron Radiation Facility

■ REFERENCES

- (1) Kouzarides, T. Chromatin modifications and their function. *Cell* **2007**, *128* (4), 693–705.
- (2) Bannister, A. J.; Kouzarides, T. Regulation of chromatin by histone modifications. *Cell Res.* **2011**, *21* (3), 381–395.
- (3) (a) Rando, O. J. Combinatorial complexity in chromatin structure and function: revisiting the histone code. *Curr. Opin. Genet. Dev.* **2012**, *22* (2), 148–155. (b) Jenuwein, T.; Allis, C. D. Translating the histone code. *Science* **2001**, *293* (5532), 1074–1080. (c) Strahl, B. D.; Allis, C. D. The language of covalent histone modifications. *Nature* **2000**, *403* (6765), 41–45.
- (4) (a) Lorenzen, J. M.; Martino, F.; Thum, T. Epigenetic modifications in cardiovascular disease. *Basic Res. Cardiol.* **2012**, *107* (2), 245. (b) Arrowsmith, C. H.; Bountra, C.; Fish, P. V.; Lee, K.; Schapira, M. Epigenetic protein families: a new frontier for drug discovery. *Nat. Rev. Drug Discovery* **2012**, *11* (5), 384–400. (c) Dawson, M. A.; Kouzarides, T. Cancer epigenetics: from mechanism to therapy. *Cell* **2012**, *150* (1), 12–27. (d) Chi, P.; Allis, C. D.; Wang, G. G. Covalent histone modifications—miswritten, misinterpreted and mis-erased in human cancers. *Nat. Rev. Cancer* **2010**, *10* (7), 457–469.
- (5) (a) Furdas, S. D.; Carlino, L.; Sippl, W.; Jung, M. Inhibition of bromodomain-mediated protein–protein interactions as a novel

- therapeutic strategy. *MedChemComm* **2012**, 3 (2), 123–134. (b) Filippakopoulos, P.; Picaud, S.; Mangos, M.; Keates, T.; Lambert, J. P.; Baryte-Lovejoy, D.; Felletar, I.; Volkmer, R.; Muller, S.; Pawson, T.; Gingras, A. C.; Arrowsmith, C. H.; Knapp, S. Histone recognition and large-scale structural analysis of the human bromodomain family. *Cell* **2012**, 149 (1), 214–231. (c) Hewings, D. S.; Rooney, T. P. C.; Jennings, L. E.; Hay, D. A.; Schofield, C. J.; Brennan, P. E.; Knapp, S.; Conway, S. J. Progress in the development and application of small molecule inhibitors of bromodomain-acetyl-lysine interactions. *J. Med. Chem.* **2012**, 55 (22), 9393–9413.
- (6) Prinjha, R. K.; Witherington, J.; Lee, K. Place your BETs: the therapeutic potential of bromodomains. *Trends Pharmacol. Sci.* **2012**, 33 (3), 146–153.
- (7) Filippakopoulos, P.; Qi, J.; Picaud, S.; Shen, Y.; Smith, W. B.; Fedorov, O.; Morse, E. M.; Keates, T.; Hickman, T. T.; Felletar, I.; Philpott, M.; Munro, S.; McKeown, M. R.; Wang, Y. C.; Christie, A. L.; West, N.; Cameron, M. J.; Schwartz, B.; Heightman, T. D.; La Thangue, N.; French, C. A.; Wiest, O.; Kung, A. L.; Knapp, S.; Bradner, J. E. Selective inhibition of BET bromodomains. *Nature* **2010**, 468 (7327), 1067–1073.
- (8) French, C. A.; Ramirez, C. L.; Kolmakova, J.; Hickman, T. T.; Cameron, M. J.; Thyne, M. E.; Kutok, J. L.; Toretsky, J. A.; Tadavarthy, A. K.; Kees, U. R.; Fletcher, J. A.; Aster, J. C. BRD-NUT oncoproteins: a family of closely related nuclear proteins that block epithelial differentiation and maintain the growth of carcinoma cells. *Oncogene* **2008**, 27 (15), 2237–2242.
- (9) Qi, J.; Filippakopoulos, P.; Picaud, S.; Smith, W.; Keates, T.; Morse, E.; Philpott, M.; Shaw, K.; Fedorov, O.; West, N.; Heightman, T.; French, C.; Knapp, S.; Bradner, J. Small-molecule bromodomain inhibitors for cancer therapy. *Abstr. Pap.—Am. Chem. Soc.* **2010**, 240.
- (10) Muller, S.; Filippakopoulos, P.; Knapp, S. Bromodomains as therapeutic targets. *Expert Rev. Mol. Med.* **2011**, 13, 1–21.
- (11) (a) Chung, C. W.; Coste, H.; White, J. H.; Mirguet, O.; Wilde, J.; Gosmini, R. L.; Delves, C.; Magny, S. M.; Woodward, R.; Hughes, S. A.; Boursier, E. V.; Flynn, H.; Bouillot, A. M.; Bamborough, P.; Brusq, J. M. G.; Gellibert, F. J.; Jones, E. J.; Riou, A. M.; Homes, P.; Martin, S. L.; Uings, I. J.; Toum, J.; Clement, C. A.; Boullay, A. B.; Grimley, R. L.; Blande, F. M.; Prinjha, R. K.; Lee, K.; Kirilovsky, J.; Nicodeme, E. Discovery and characterization of small molecule inhibitors of the BET family bromodomains. *J. Med. Chem.* **2011**, 54 (11), 3827–3838. (b) Nicodeme, E.; Jeffrey, K. L.; Schaefer, U.; Beinke, S.; Dewell, S.; Chung, C. W.; Chandwani, R.; Marazzi, I.; Wilson, P.; Coste, H.; White, J.; Kirilovsky, J.; Rice, C. M.; Lora, J. M.; Prinjha, R. K.; Lee, K.; Tarakhovskiy, A. Suppression of inflammation by a synthetic histone mimic. *Nature* **2010**, 468 (7327), 1119–1123.
- (12) Matzuk, M. M.; McKeown, M. R.; Filippakopoulos, P.; Li, Q. L.; Ma, L.; Agno, J. E.; Lemieux, M. E.; Picaud, S.; Yu, R. N.; Qi, J.; Knapp, S.; Bradner, J. E. Small-molecule inhibition of BRDT for male contraception. *Cell* **2012**, 150 (4), 673–684.
- (13) Stelow, E. B. A review of NUT midline carcinoma. *Head Neck Pathol* **2011**, 5 (1), 31–5.
- (14) (a) Hewings, D. S.; Wang, M. H.; Philpott, M.; Fedorov, O.; Uttarkar, S.; Filippakopoulos, P.; Picaud, S.; Vuppasetty, C.; Marsden, B.; Knapp, S.; Conway, S. J.; Heightman, T. D. 3,5-Dimethylisoxazoles act as acetyl-lysine-mimetic bromodomain ligands. *J. Med. Chem.* **2011**, 54 (19), 6761–6770. (b) Dawson, M. A.; Prinjha, R. K.; Dittmann, A.; Giotopoulos, G.; Bantscheff, M.; Chan, W. I.; Robson, S. C.; Chung, C. W.; Hopf, C.; Savitski, M. M.; Huthmacher, C.; Gudgin, E.; Lugo, D.; Beinke, S.; Chapman, T. D.; Roberts, E. J.; Soden, P. E.; Auger, K. R.; Mirguet, O.; Doehner, K.; Delwel, R.; Burnett, A. K.; Jeffrey, P.; Drewes, G.; Lee, K.; Huntly, B. J. P.; Kouzarides, T. Inhibition of BET recruitment to chromatin as an effective treatment for MLL-fusion leukaemia. *Nature* **2011**, 478 (7370), 529–533.
- (15) (a) Chung, C. W.; Dean, A. W.; Woolven, J. M.; Bamborough, P. Fragment-based discovery of bromodomain inhibitors part 1: inhibitor binding modes and implications for lead discovery. *J. Med. Chem.* **2012**, 55 (2), 576–586. (b) Bamborough, P.; Diallo, H.; Goodacre, J. D.; Gordon, L.; Lewis, A.; Seal, J. T.; Wilson, D. M.; Woodrow, M. D.; Chung, C. W. Fragment-based discovery of bromodomain inhibitors part 2: optimization of phenylisoxazole sulfonamides. *J. Med. Chem.* **2012**, 55 (2), 587–596.
- (16) Murray, C. W.; Rees, D. C. The rise of fragment-based drug discovery. *Nat. Chem.* **2009**, 1 (3), 187–192.
- (17) Congreve, M.; Carr, R.; Murray, C.; Jhoti, H. A rule of three for fragment-based lead discovery? *Drug Discovery Today* **2003**, 8 (19), 876–877.
- (18) Lipinski, C. A.; Lombardo, F.; Dominy, B. W.; Feeney, P. J. Experimental and computational approaches to estimate solubility and permeability in drug discovery and development settings. *Adv. Drug Delivery Rev.* **1997**, 23 (1–3), 3–25.
- (19) (a) Chen, I. J.; Hubbard, R. E. Lessons for fragment library design: analysis of output from multiple screening campaigns. *J. Comput.-Aided Mol. Des.* **2009**, 23 (8), 603–620. (b) Hubbard, R. E.; Davis, B.; Chen, I.; Drysdale, M. J. The SeedS approach: integrating fragments into drug discovery. *Curr. Top. Med. Chem.* **2007**, 7 (16), 1568–1581.
- (20) Venhorst, J.; Nunez, S.; Kruse, C. G. Design of a high fragment efficiency library by molecular graph theory. *ACS Med. Chem. Lett.* **2010**, 1 (9), 499–503.
- (21) Weber, L. JChem Base—ChemAxon. *Chem. World* **2008**, 5 (10), 65–66.
- (22) Scott, D. E.; Coyne, A. G.; Hudson, S. A.; Abell, C. Fragment-based approaches in drug discovery and chemical biology. *Biochemistry* **2012**, 51 (25), 4990–5003.
- (23) Niesen, F. H.; Berglund, H.; Vedadi, M. The use of differential scanning fluorimetry to detect ligand interactions that promote protein stability. *Nat. Protoc.* **2007**, 2 (9), 2212–2221.
- (24) Mayer, M.; Meyer, B. Characterization of ligand binding by saturation transfer difference NMR spectroscopy. *Angew. Chem., Int. Ed.* **1999**, 38 (12), 1784–1788.
- (25) Dalvit, C.; Fogliatto, G.; Stewart, A.; Veronesi, M.; Stockman, B. WaterLOGSY as a method for primary NMR screening: practical aspects and range of applicability. *J. Biomol. NMR* **2001**, 21 (4), 349–359.
- (26) Loria, J. P.; Rance, M.; Palmer, A. G. A relaxation-compensated Carr–Purcell–Meiboom–Gill sequence for characterizing chemical exchange by NMR spectroscopy. *J. Am. Chem. Soc.* **1999**, 121 (10), 2331–2332.
- (27) Navratilova, I.; Hopkins, A. L. Fragment screening by surface plasmon resonance. *ACS Med. Chem. Lett.* **2010**, 1 (1), 44–48.
- (28) Philpott, M.; Yang, J.; Tumber, T.; Fedorov, O.; Uttarkar, S.; Filippakopoulos, P.; Picaud, S.; Keates, T.; Felletar, I.; Ciulli, A.; Knapp, S.; Heightman, T. D. Bromodomain-peptide displacement assays for interactome mapping and inhibitor discovery. *Mol. Biosyst.* **2011**, 7 (10), 2899–2908.
- (29) Caldwell, G. W.; Yan, Z. Y.; Tang, W. M.; Dasgupta, M.; Hasting, B. ADME optimization and toxicity assessment in early- and late-phase drug discovery. *Curr. Top. Med. Chem.* **2009**, 9 (11), 965–980.
- (30) (a) Sutherland, J. J.; Raymond, J. W.; Stevens, J. L.; Baker, T. K.; Watson, D. E. Relating molecular properties and in vitro assay results to in vivo drug disposition and toxicity outcomes. *J. Med. Chem.* **2012**, 55 (14), 6455–6466. (b) Waring, M. J. Defining optimum lipophilicity and molecular weight ranges for drug candidates—molecular weight dependent lower logD limits based on permeability. *Bioorg. Med. Chem. Lett.* **2009**, 19 (10), 2844–2851. (c) Winiwarter, S.; Bonham, N. M.; Ax, F.; Hallberg, A.; Lennernas, H.; Karlen, A. Correlation of human jejunal permeability (in vivo) of drugs with experimentally and theoretically derived parameters. A multivariate data analysis approach. *J. Med. Chem.* **1998**, 41 (25), 4939–4949.
- (31) Friesner, R. A.; Murphy, R. B.; Repasky, M. P.; Frye, L. L.; Greenwood, J. R.; Halgren, T. A.; Sanschagrin, P. C.; Mainz, D. T. Extra precision glide: docking and scoring incorporating a model of hydrophobic enclosure for protein–ligand complexes. *J. Med. Chem.* **2006**, 49 (21), 6177–6196.
- (32) Halgren, T. A.; Murphy, R. B.; Friesner, R. A.; Beard, H. S.; Frye, L. L.; Pollard, W. T.; Banks, J. L. Glide: a new approach for rapid, accurate docking and scoring. 2. Enrichment factors in database screening. *J. Med. Chem.* **2004**, 47 (7), 1750–1759.

- (33) Otwinowski, Z.; Minor, W. Processing of X-ray diffraction data collected in oscillation mode. *Methods Enzymol.* **1997**, *276*, 307–326.
- (34) Murshudov, G. N.; Vagin, A. A.; Dodson, E. J. Refinement of macromolecular structures by the maximum-likelihood method. *Acta Crystallogr., Sect. D* **1997**, *53*, 240–255.
- (35) Adams, P. D.; Grosse-Kunstleve, R. W.; Hung, L. W.; Ioerger, T. R.; McCoy, A. J.; Moriarty, N. W.; Read, R. J.; Sacchettini, J. C.; Sauter, N. K.; Terwilliger, T. C. PHENIX: building new software for automated crystallographic structure determination. *Acta Crystallogr., Sect. D* **2002**, *58*, 1948–1954.
- (36) Emsley, P.; Lohkamp, B.; Scott, W. G.; Cowtan, K. Features and development of Coot. *Acta Crystallogr., Sect. D* **2010**, *66*, 486–501.
- (37) Manzo, S. G.; Zhou, Z. L.; Wang, Y. Q.; Marinello, J.; He, J. X.; Li, Y. C.; Ding, J.; Capranico, G.; Miao, Z. H. Natural product triptolide mediates cancer cell death by triggering CDK7-dependent degradation of RNA polymerase II. *Cancer Res.* **2012**, *72* (20), 5363–5373.